DOI: 10.1070/RCR4720

Kinetics of formation and dissociation of gas hydrates

Andrey Yu. Manakov,[a] Nikita V. Penkov,[b] Tatyana V. Rodionova,[a] Anatoliy N. Nesterov,[c, d] Evgeny E. Fesenko Jr. [b]

[a] Nikolaev Institute of Inorganic Chemistry, Siberian Branch of the Russian Academy of Sciences prosp. Akademika Lavrentieva 3, 630090 Novosibirsk, Russian Federation
[b] Institute of Cell Biophysics, Russian Academy of Sciences ul. Institutskaya 3, 142290 Pushchino, Moscow Region, Russian Federation
[c] Institute of Earth Cryosphere, Siberian Branch of the Russian Academy of Sciences ul. Malygina 86, 625026 Tyumen, Russian Federation
[d] Tyumen State University ul. Volodarskogo 6, 625003 Tyumen, Russian Federation

The review covers a wide range of issues related to the nucleation, growth and dissociation of gas hydrates. The attention is focused on publications of the last 10 – 15 years. Along with the mathematical models used to describe these processes, the results of relevant experimental studies are surveyed. Particular sections are devoted to the gas hydrate self-preservation effect, the water memory effect in the hydrate formation, development of catalysts for hydrate formation and the effect of substances dissolved in the aqueous phase on the formation of hydrates. The main experimental techniques used to study gas hydrates are briefly considered.
The bibliography includes 230 references.

Contents

I. Introduction 845
II. Nucleation of gas hydrates 848
III. Growth and dissociation of gas hydrates 856
IV. Methods for studying the formation and dissociation kinetics of gas hydrates 864
V. Conclusion 866

I. Introduction

I.1. Natural and man-made gas hydrates

Gas hydrates are white, ice-like substances, the crystalline framework of which (host framework) is composed of water molecules linked to one another by hydrogen bonds. The framework contains cavities (cages), which accommodate molecules of another sort — guest molecules. The guest molecules in gas hydrates can be represented by inert gas atoms, lower hydrocarbon molecules, Freon molecules, some organic solvents and so on. As a rule, gas hydrates are stable below room temperature at elevated pressure. One volume of a gas hydrate can hold up to 170 volumes of a gas (0.1 MPa and 273.15 K). Detailed information on various gas hydrate-related issues is available from publications.[1 – 4]

A.Yu.Manakov. Dr.Sci. (Chem.), Chief Researcher, Head of the Laboratory of Clathrate Compounds at the NIIC SB RAS.
Telephone: +7(383)316 – 5346, e-mail: manakov@niic.nsc.ru
Current research interests: structure, composition and properties of clathrate hydrates.
N.V.Penkov. Ph.D. (Phys.-Math.), Senior Researcher of the Laboratory of Cryobiology and Water Biophysics at the ICB RAS.
Telephone: +7(4967)739 – 511, e-mail: nvpenkov@yandex.ru
Current research interests: spectroscopy of aqueous solutions, photon correlation spectroscopy.
T.V.Rodionova. Ph.D. (Chem.), Senior Researcher of the Laboratory of Clathrate Compounds at the NIIC SB RAS.
Telephone: +7(383)316 – 5346, e-mail: tvr@niic.nsc.ru
Current research interests: structure, composition and properties of clathrate hydrates.
A.N.Nesterov. Dr.Sci. (Chem.), Deputy Director for Science of the IEC SB RAS, Leading Researcher at the TyumSU.
Telephone: +7(3452)688 – 722, e-mail: nesterov@ikz.ru
Current research interests: phase equilibria and transitions in hydrocarbon systems, gas hydrates.
E.E.Fesenko Jr. Ph.D. (Biol.), Head of the Laboratory of Cryobiology and Water Biophysics at the ICB RAS.
Telephone: +7(4967)739 – 212, e-mail: eugenyfesenko@yandex.ru
Current research interests: cryobiology, biophysics of aqueous solutions.

Received 30 December 2016
Translation: Z.P.Svitanko

© 2017 Russian Academy of Sciences and Turpion Ltd.

Natural gas hydrates were discovered by Soviet scientists in the 1960s.[5] These compounds are very sensitive to pressure and temperature changes in the upper parts of the Earth's crust. For gas hydrates to exist in Nature, the following conditions are required: high pressure, relatively low temperature, the presence of water and a free (or dissolved) hydrate-forming gas in contact with water. The major hydrate-forming gas is methane. In accumulations of natural gas hydrates formed by the biogenic gas, the proportion of methane is 98%–99%, the other possible components being ethane, propane, butane, carbon dioxide, hydrogen sulfide, nitrogen, *etc*. In the hydrates formed by catagenetic gas, the content of these impurities can reach tens of percent.

In Nature, hydrates can occur in the sediments of oceans, seas and even deep fresh-water bodies (such as Lake Baikal), as well as in permafrost rocks. The minimum water depth suitable for the occurrence of hydrates in the bottom sediments is ~300 m for the Arctic continental shelf and 400 m for other areas. The hydrate stability zone (HSZ) in sea sediments can be up to a kilometre thick. In permafrost rocks, the minimum depth of the HSZ upper boundary is about 200 m, with the HSZ thickness being 400–800 m (in some cases, >1 km).The so-called relic gas hydrate accumulations,[1] which have been preserved in the frozen rock outside the thermodynamic stability zone, can occur above the HSZ. The morphology of gas hydrate inclusions in the rock can be quite diverse, ranging from thick (tens of centimetres) monolithic layers to small lenses.[1,6] Also, gas hydrates do not necessarily form macroscopic inclusions, but may occur in the pore space of the rock as a sort of hydrate cement.[6] In this case, the hydrate-forming rock behaves as frozen soil even at temperatures >273 K. Detailed information about the occurrence and the history of discovery of natural gas hydrates is available from the literature.[1,2,6–8]

The most recent estimates of natural gas resources existing as gas hydrates[9,10] vary from 2×10^{14} to 5×10^{15} m^3, which is at least comparable with the explored resources of conventional natural gas. The estimates of hydrate gas resources in permafrost rocks[11] in Russia made by specialists of the Research Institute of Natural Gases and Gas Technologies (VNIIGAZ) vary from 7.2×10^{12} to 1.7×10^{13} m^3. The experimental gas production from hydrate accumulations took place in the permafrost zone (Mallik gas hydrate site, at the moth of the Mackenzie river in the north of Canada) in 2002–2009 and in the continental slope of the eastern Nankai Trough (off the south-eastern coast of Japan) in 2013.[12] However, the first experience of gas production from gas hydrates probably dates back to the period of development of the Messoyakha oil and gas field in West Siberia (production started in 1970).

Currently, apart from the resource issues, natural gas hydrates are considered as participants of global processes associated with climatic changes. Also, man-made gas hydrate formation plays (or can play) an important role in some fields of science and technology, the key of which are as follows.

Prevention of hydrate formation. This is an issue for the production and transportation of natural gas and oil, especially for offshore fields and cold climate zones.[2–4] Most often, this is done using thermodynamic inhibitors (methanol, glycols, salt solutions and composites), which, being dissolved in water, shift the conditions of hydrate formation to lower temperatures and higher pressures.†

Gas storage and transportation in the gas hydrate form.[13,14] The most significant results along this line were obtained by the Mitsui Engineering and Shipbuilding company, which developed process flows for marine transportation of natural gas hydrate from Southeast Asia fields to Japan. A hydrate production unit with a design capacity of up to 5000 kg per day was constructed and the demonstration project on gas delivery as the hydrate to the end consumer was successfully implemented.

Gas hydrates for water desalination.[15] Several large units utilizing this technology were constructed in the second half of the 20th century and were successfully operated for a long period of time.

Gas hydrates for separation of gas mixtures.[16] Specialists recognize good prospects of this approach; research in this area is in progress; however, no examples of large-scale practical implementation of this technology are available as yet.

Gas hydrates for carbon dioxide sequestration.[17] The possibility of capture of industry-produced carbon dioxide as gas hydrate on the ocean bottom is being discussed in the literature. In 2012, a large-scale field experiment on methane displacement from a gas hydrate accumulation by CO_2 was carried out.[10] This approach could be used for methane production from the hydrates simultaneously with CO_2 capture.

Gas hydrates for cryoconservation of biological specimens. This issue is at the level of discussion; the first experimental studies have been performed.[18]

I.2. Brief information about the molecular structure and formation processes of clathrate hydrates

The crystalline framework of gas hydrates is composed of water molecules, each being hydrogen-bonded to four neighbouring ones. The bond arrangement corresponds to a slightly distorted tetrahedron. This framework has polyhedral cavities of molecular size accessible for guest molecules. Most often, van der Waals interactions occur between the hydrate framework and the guest molecules. The gas hydrate frameworks are usually represented as a packing of such polyhedral cavities; the vertices of the polyhedra correspond to oxygen atoms and the edges are hydrogen bonds. The neighbouring polyhedra share faces and are thus connected into an infinite three-dimensional framework. The hydrate framework by itself is thermodynamically unstable; it is stable only if a certain proportion of cavities are filled with guest molecules. At moderate pressures (up to 100 MPa), each cavity accommodates, as a rule, not more than one guest molecule.

Polyhedral cavities with 12, 14, 16 and 20 faces, which are designated by letters D (D'), T, H and E, respectively, are encountered most often in hydrate frameworks (Fig. 1).

† In recent years, so-called low-dosage hydrate inhibitors have been finding increasing use in the oil industry. They are called so because the consumption rates of these inhibitors are an order of magnitude lower than those for thermodynamic inhibitors. Low-dosage inhibitors include kinetic inhibitors, which extend the induction time of hydrate formation, and anti-agglomerants, which do not interfere with hydrate formation, but prevent the hydrate particles from aggregation and formation of hydrate plugs.

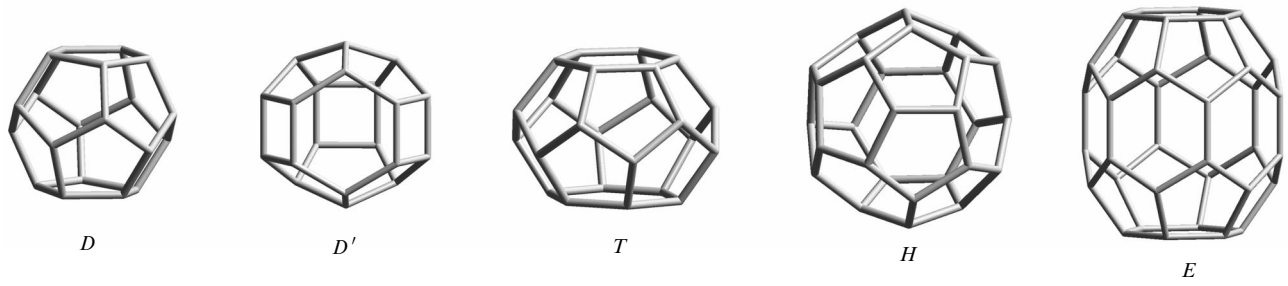


Figure 1. Typical cavities in the frameworks of gas hydrates.

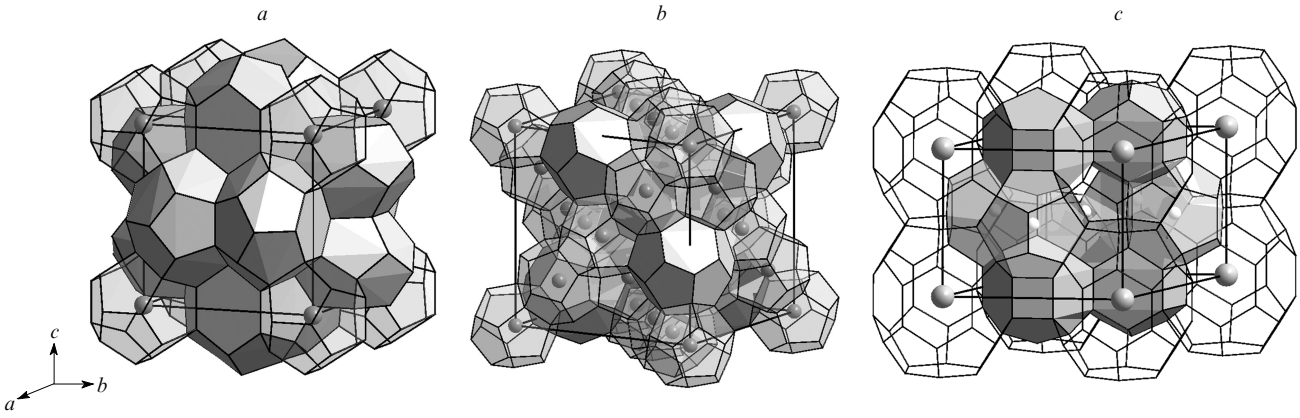


Figure 2. Packing of cavities in the frameworks of sI (*a*), sII (*b*) and sH (*c*) hydrates. The spheres designate the visible cavity centres. Drawn on the basis of Refs 1 and 2.

According to their sizes, the cavities *D* and *D′* are called small and the other cavities are called large. The vast majority of known gas hydrates refer to either of two structures, cubic structure I (below referred to sI) and cubic structure II (below referred to as sII). In the case of large hydrate-forming molecules (adamantane, methylcyclohexane and so on) in the presence of a second hydrate-forming agent (help gas), hydrates based on hexagonal structure III (below referred to as sH) can be formed (Fig. 2). Some characteristics of gas hydrate frameworks are summarized in Table 1. Detailed information about the hydrate structures can be found in the literature.[1–4] New gas hydrate frameworks existing at high pressures have been considered.[19]

The type of the hydrate structure to be formed is determined by the nature of guest molecule; in the case of a mixture of guest components, it is determined by the composition of this mixture. Usually, large cavities in the hydrate frameworks are almost completely filled by guest molecules, only 1% – 2% of such cavities remaining vacant; therefore, their occupancy can be taken to be 1. The occupancy of small cavities is variable (from 0 to 1) and increases with increasing pressure. For pressures <100 MPa, multiple filling of small cavities (several guest molecules in one cavity) was not observed. Gases with molecule (atom) sizes from 3.5 to 4.2 Å (Ar, Kr, N_2, O_2) form sII hydrates. The limiting composition of these hydrates is 24 guest molecules per 136 water molecules per unit cell (see Table 1), *i.e.*, $G \cdot 5^2/_3 H_2O$ (here and below, G stands for the guest). Hydrates with the sI structure are formed by 4.3 to 5.8 Å molecules (CH_4, H_2S, CO_2, SO_2, Xe, C_2H_6. *etc.*). In this case, the hydrate composition can vary from $G \cdot 7^2/_3 H_2O$ (only *T*-cavities are occupied) to $G \cdot 5.75 H_2O$ (all *D*- and *T*-cavities are occupied). If the

Table 1. Characteristics of the mot frequently occurring structures of the aqueous frameworks of gas hydrates.[1,2]

Structure	Space group	Unit cell formula	Unit cell parameters /Å	Density of the vacant framework /g cm^{-3}	n_w (see[a])
sI	$Pm\bar{3}n$	$6\,T \cdot 2\,D \cdot 46\,H_2O$	$a = 12.0$	0.796	5.75[b] 7.67[c]
sII	$Fd\bar{3}m$	$8\,H \cdot 16\,D \cdot 136\,H_2O$	$a = 17.1$	0.812	5.67[b] 17[c]
sH	$P6/mmm$	$E \cdot 2\,D' \cdot 3\,D \cdot 34\,H_2O$	$a = 12.3$, $c = 10.2$	0.768	34[d]

[a] n_w is the hydrate number, *i.e.*, the number of water molecules per guest molecule in the hydrate. [b] Small and large cavities are occupied. [c] Only large cavities are occupied. [d] Hydrates are not formed without an help guest; the formula is usually written in relation to 34 water molecules.

size of the guest molecule is in the 5.8–7.2 Å range (CCl_4, THF, C_3H_8, SF_6), sII hydrates are formed, with only large cavities being filled, *i.e.*, the hydrate composition is $G \cdot 17\,H_2O$.

Clathrate hydrates formed by mixtures of two or more types of guest molecules are usually called binary or mixed. In the simple case if both components of the mixture form hydrates of the same structure, the binary hydrate is a continuous solid solution with the same structural type. For example, in the case of a mixture of CH_4 and CO_2, hydrates with sI structure are formed at any component concentrations. The behaviour of the methane–ethane–water system is much more intricate: mixtures with methane contents of 61%–93% form sII hydrates, while mixtures with other compositions form sI hydrates. If the size of the guest molecule is in the range of 7.2–9.0 Å, binary sH hydrates can be formed in the presence of auxiliary components. At moderate pressure ($\sim$2 MPa), large cavities in the hydrates with this type of structure are occupied by a large molecule (adamantane, methylcyclohexane, 2,2-dimethylpentane and so on) that does not form individual clathrate hydrates, while small cavities are occupied by H_2S, Xe or CH_4 molecules. The limiting composition of these hydrates corresponds to the formula $G_2 \cdot 5\,G_1 \cdot 34\,H_2O$ (G_1 is guest in small cavities, G_2 is guest in large cavities). The occupancy of small cavities with an auxiliary gas is, as a rule, <1.

In order to describe the conditions of existence of gas hydrates in hydrate-forming component–water binary systems, $P-T$ projections of the corresponding phase diagrams are used (Fig. 3).[1–4] They represent sets of lines that confine the existence region of the hydrate. The lines correspond to the phases that occur in equilibrium under these conditions.

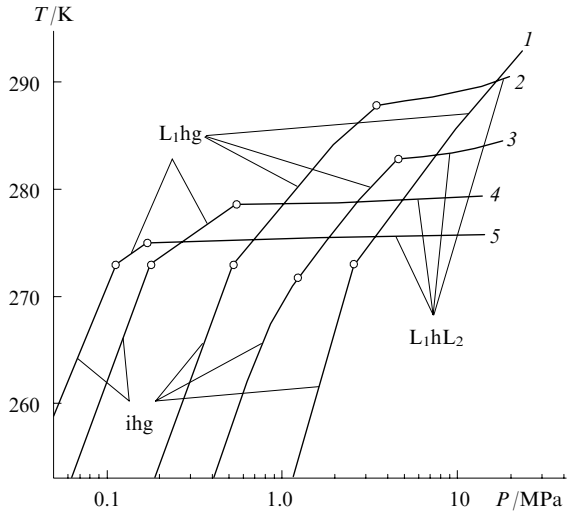


Figure 3. $P-T$ projections of phase diagrams of some gas–water systems. Drawn on the basis of Refs 1 and 2.
Gas: (*1*) CH_4, (*2*) C_2H_6, (*3*) CO_2, (*4*) C_3H_8, (*5*) *i*-C_4H_{10}; quadruple points for the systems are shown; g is gas, h is hydrate, L_1, L_2 are a liquid water and hydrate-forming component, respectively; i is ice, ihg is the ice–hydrate–gas equilibrium; L_1hg is the liquid water–hydrate–gas equilibrium; L_1hL_2 is the liquid water–hydrate–liquid hydrate-forming component equilibrium; here and below by liquid water is meant a solution of hydrate-forming gas in water saturated under the given conditions.

Several types of hydrate formation and dissociation processes can be distinguished, depending on the physical state of the reactants and reaction products involved. Most detailed kinetic studies have been done for the formation of thermodynamically stable hydrates from liquid water and a hydrate-forming gas and for hydrate dissociation to liquid water and a gas. Instead of a gas, liquid hydrate-forming components (Freons, CCl_4 and so on) are possible. Below water freezing point, a thermodynamically stable hydrate can be formed from ice and a gas or from ice and metastable liquid water. Correspondingly, these phases can be formed upon dissociation of this hydrate.

Metastable hydrates can be obtained from supercooled water in the absence of ice.[20] The formation of gas hydrates from homogeneous aqueous solutions of gases is frequently encountered in Nature. It is difficult to reproduce these processes in a laboratory; therefore, they are modelled using solutions of THF in water.

Currently, natural and man-made gas hydrates represent a topical and vigorously developing investigation area. The practical importance of research in this area is also beyond doubt. Analysis of relevant literature has shown that in the last 10–15 years, the greatest advances were made in the studies of gas hydrate formation and dissociation kinetics. The 'engineering' approach to the description of gas hydrates, which prevailed in early studies, was replaced by up-to-date scientific approaches. This review surveys the studies dealing with gas hydrate nucleation and gas hydrate growth and dissociation kinetics carried out mainly in the last 15 years.

II. Nucleation of gas hydrates

II.1. Nucleation of gas hydrates from liquid water and gas

The formation of a new phase comprises two key stages: appearance of stable nuclei of a new phase (nucleation) and their growth. According to the classical nucleation theory, the appearance of a stable phase in a metastable parent phase (supercooled or superheated liquid, supercooled gas, *etc.*) requires the formation of a tiny particle (nucleus) of the stable phase able to grow by itself. When a gas hydrate is formed from liquid water and a gas, the nucleation occurs most often near the gas/liquid interface.[1,2,21–23] It is assumed that the maximum supersaturation of the liquid with dissolved gas and the highest water vapour concentration in the gas phase occur in this region. This assumption was confirmed in independent experiments. The presence of a guest-enriched layer at the carbon dioxide/water and xenon/water interfaces was shown by Boewer *et al.*[24] No such layer was found in the propane/water and isobutane/water systems. The authors demonstrated that hydrates are formed more rapidly in the former two systems. It is noteworthy that the nucleation of the hydrate in the bulk liquid phase is not prohibited, but only requires a sufficient supersaturation of the solution (for example, by means of a local temperature decrease). Several recent reviews present detailed surveys of the papers on numerical simulation of the nucleation processes.[25,26] Below we mainly discuss the results of experimental studies.

The notion of hydrate nucleation is closely connected with the view on the structures of water and aqueous solutions of hydrophobic compounds. Currently, it is believed that most of water molecules in the liquid phase are involved in a 3D network of hydrogen bonds and that

fragments of snapshot configurations of these bonds have features in common with structures of ice.[27] These configurations are very rapidly interconverted as a result of rotational and translational motion of water molecules. The degree of structuring of liquid water decreases with increasing temperature and pressure.[28] Upon dissolution of hydrophobic substances, water molecules cannot form bonds with solute molecules, which results in local disruption of the hydrogen bond network. As this takes place, water molecules rearrange and form a sort of cage around the solute molecule, the inner surface of the cage being formed by water molecules with hydrogen bonds mainly directed tangentially to the surface of the hydrophobic molecule.[29–31] The resulting cage is a disordered analogue of the cavities in clathrate hydrates.[32] According to the most common hydrate formation model,[2] agglomerates of these cavities are the building units of the hydrate lattice. As the temperature decreases, they stick together in the vicinity of the gas/liquid interface to give the hydrate precursor (Fig. 4).

It was shown by Raman spectroscopy and powder X-ray diffraction[33,34] that in early stages of hydrate formation, the methane hydrate phase being formed is non-crystalline and contains mainly small cavities. The initial amorphous phase is transformed into the crystalline hydrate in the later stages of hydrate formation. The nucleation near the interface and appearance of amorphous seeds were simulated in a theoretical study.[35] Calculations showed[36] the possibility of both direct crystallization of the hydrate and two-stage hydrate formation involving the amorphous phase. An alternative view on the mechanism of hydrate nucleation was developed relying on the results of a number of publications.[37–41] The mechanism considered in these works can be described in the simplified form as simultaneous ordering of some group of adjacent gas and water molecules to give a clathrate-like structure. This process can be facilitated by accumulation of dissolved molecules of the hydrate-forming agent near the solid/liquid interface.[42] A similar model that implies the formation of a drop from guest molecules separated by water molecules in the first stage followed by transformation to the amorphous and then crystalline hydrate has also been reported.[43–46]

Two types of nucleation are distinguished:

— homogeneous nucleation, in which the primary nucleus is formed only *via* local density fluctuations in the initial metastable phase, and

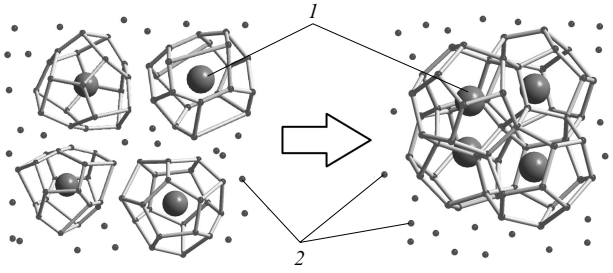


Figure 4. Scheme of methane dissolution in water with inclusion into clusters of water molecules shaped like a distorted dodecahedron (on the left) and the subsequent formation of an agglomerate of dodecahedral cavities (on the right).[2]
(*1*) Methane molecules, (*2*) oxygen atoms of water molecules; polyhedron edges stand for hydrogen bonds.

— heterogeneous nucleation, in which the primary nucleus is formed on tiny solid particles present in the liquid, active points on the reactor walls, *etc.*, which are usually called heterogeneous nucleation sites.

All other factors being the same, the homogeneous nucleation temperature corresponds to the maximum possible supercooling of the system. The control over the existing nucleation sites is an unsolved issue, because it is impossible to completely remove heterogeneous impurities from the liquid and to eliminate the contact with reactor walls, ingress of particles from air into the liquid, detachment of microparticles from the reactor walls and so on.

By a nucleus of the nascent phase is meant a nano-sized entity consisting of as few as tens or hundreds of unit cells. The application of the classical nucleation theory to gas hydrate formation has been reported by Kashchiev and Firoozabadi.[47,48] The authors assumed that the hydrate is formed *via* coalescence of similar building units described as $G \cdot n_w H_2O$. In this case, the work W (in J) for the formation of a nucleus consisting of n building units can be expressed by the relation

$$W(n) = -n\Delta\mu + c\sigma_{ef}(\upsilon_h n)^{2/3} \quad (1)$$

where $\Delta\mu$ is the gain of the volume free energy upon transition of one building unit from the supercooled phase to the hydrate ($\Delta\mu > 0$ determines the driving force of hydrate formation) /J; c is the geometric factor characterizing the shape of nucleus; σ_{ef} is the effective specific surface energy of the nucleus /J m^{-2}; υ_h is the volume of one building unit /m^3. The first term in the relation characterizes the volume energy and the second term characterizes the surface energy of the nucleus.

The shape of the curve illustrating the dependence of the nucleus energy on the number of building units in it is shown in Fig. 5. The particular expressions for the driving force of hydrate formation are as follows:

for an isothermal process,

$$\Delta\mu = kT\ln\frac{f}{f_{eq}} + \Delta\upsilon_e(P - P_{eq}) \quad (2)$$

for an isobaric process,

$$\Delta\mu = \Delta S_e \Delta T \quad (3)$$

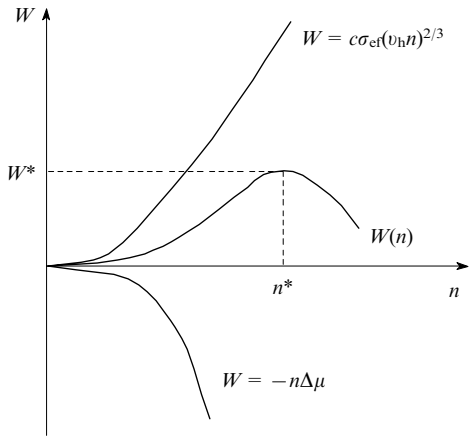


Figure 5. Work done to form the gas hydrate nucleus *vs.* the number of building units in the nucleus.[47]

Here f, P and f_{eq}, P_{eq} are the fugacity and pressure of the hydrate-forming gas, respectively, under the given conditions and at the equilibrium hydrate formation temperature T_{eq}; Δv_e is the difference between the volumes of n_w water molecules in the solution and in the hydrate building unit in the hydrate crystal /m^3; ΔS_e is the entropy change upon hydrate formation /J K^{-1}; ΔT is the supercooling /K ($\Delta T = T_{eq} - T$); k is the Boltzmann constant /J K^{-1}.

The σ_{ef} value in Eqn (1) depends on the nucleus position. In the case of homogeneous nucleation, the whole nucleus occurs in the bulk of the liquid and $\sigma_{ef} = \sigma$ (σ is the specific surface energy of the hydrate/liquid interface). If the nucleation is heterogeneous, $\sigma_{ef} = \Psi\sigma$, where the coefficient Ψ can vary from 0 to 1 depending on the ratio of the specific surface energies of the interfaces between contacting phases (hydrate/liquid, hydrate/solid, solid/liquid). In particular, for a hydrate nucleus shaped like a spherical segment that formed at the interface between an aqueous solution of a gas and a flat surface of a solid particle (Fig. 6), $\Psi = [0.25(2+\cos\theta)(1-\cos\theta)^2]^{1/3}$, where θ is the contact angle, which varies in the range $0 < \theta < 180^\circ$. It follows from the Young's equation that $\cos\theta = (\sigma_{s/L} - \sigma_{h/s})/\sigma$ (here $\sigma_{s/L}$ and $\sigma_{h/s}$ are specific surface energies of the solid/liquid and hydrate/solid interfaces, respectively). The coefficient Ψ takes account of the decrease in the nucleus surface energy upon interaction with the surface of the solid particle. If the free energy of the interface between the hydrate and the solid particle is lower than the hydrate/liquid surface energy, it is favourable for the hydrate nucleus to contact with the solid surface as if the hydrate wetted the surface. The degree of wetting and, hence, of the decrease in the specific surface energy of the nucleus, is characterized by the angle θ. When $\theta = 0^\circ$, then $\Psi = 0$, *i.e.*, the surface energy no longer makes a contribution to the nucleus free energy. When $\theta = 180^\circ$, then $\Psi = 1$ and, hence, it is more favourable for the hydrate to form in the liquid bulk. This corresponds to the case of homogeneous nucleation. Generally, the smaller the angle θ, the more probable the heterogeneous nucleation.

The $W(n)$ plot shown in Fig. 5 has a maximum with the coordinates n^* and W^*,

$$n^* = \frac{8c^3\sigma_{ef}^3 v_h^2}{27\Delta\mu^3} \tag{4}$$

$$W^* = \frac{4c^3\sigma_{ef}^3 v_h^2}{27\Delta\mu^2} \tag{5}$$

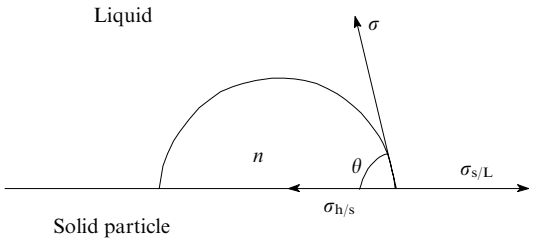


Figure 6. Chart of formation of the hydrate nucleus from n building units in a supersaturated aqueous solution of the gas on the flat surface of a solid particle (heterogeneous nucleation site).[47] The arrows mark the directions of surface tension forces.

The n^* value corresponds to the number of building units in the so-called critical nucleus and determines the nucleus size; W^* is the work done to form the critical nucleus, or the activation energy of hydrate formation.

The hydrate nucleus appears upon a random association of several building units in the initial solution. If the nucleus size $n < n^*$, an increase in the number of building units in the nucleus results in increasing the nucleus free energy. This process is energetically unfavourable, and it is more beneficial for the nucleus to dissolve. However, if $n > n^*$, the nucleus is capable of further spontaneous growth accompanied by a decrease in the free energy (see Fig. 5).

Eqations (4) and (5) indicate a strong dependence of the n^* and W^* values on σ_{ef} and $\Delta\mu$. As the nucleus surface interacts with the active sites of impurities, the nucleus surface energy decreases, which facilitates the formation of this nucleus as a result of decreasing W^*. A similar effect is observed when $\Delta\mu$ increases. According to estimates, in the case of homogeneous hydrate nucleation, a crystalline nucleus should contain approximately 150 guest molecules and W^* is $\sim 70\,kT$. In the case of heterogeneous nucleation, these values are lower.

A key characteristic of nucleation is the nucleus formation rate (nucleation rate, J), which is defined as the number of nuclei that appear in unit volume (or on unit surface) per unit time. If there are several parallel processes of nucleation (for example, hydrate nuclei may be formed both at the interface and on the nucleation sites in the system), the nucleation rate is the sum of the rates of all involved processes.

Kashchiev and Firoozabadi[47] considered in detail the nucleations of hydrates from an aqueous solution of the hydrate-forming gas. Without considering the rather cumbersome mathematical model, we will present only the expressions for the nucleation rate. In the general case,

$$J = A\exp\left(\frac{\Delta\mu}{kT}\right)\exp\left(\frac{-4c^3\sigma_{ef}^3 v_h^2}{27kT\Delta\mu^2}\right) \tag{6}$$

where A is a constant depending on the mechanism of attachment of building units to the nucleus and on the type of nucleation /m^{-3} s^{-1} in the case of hydrate formation in the bulk and m^{-2} s^{-1} in the case of hydrate formation on the surface.

If the nucleation occurs under isothermal conditions, Eqn (6) can be written in the form

$$J = AS\exp\left(\frac{-4c^3\sigma_{ef}^3 v_h^2}{27(kT)^3(\ln S)^2}\right) \tag{7}$$

where

$$S = \frac{f}{f_{eq}}\exp\left(\frac{\Delta v_e(P - P_{eq})}{kT}\right) \tag{7a}$$

For the isobaric nucleation, it follows from Eqn (6) that

$$J = A\exp\left(\frac{\Delta S_e\Delta T}{kT}\right)\exp\left(\frac{-B}{T\Delta T^2}\right) \tag{8}$$

where

$$B = \frac{4c^3\sigma_{ef}^3 v_h^2}{27k\Delta S_e^2} \tag{8a}$$

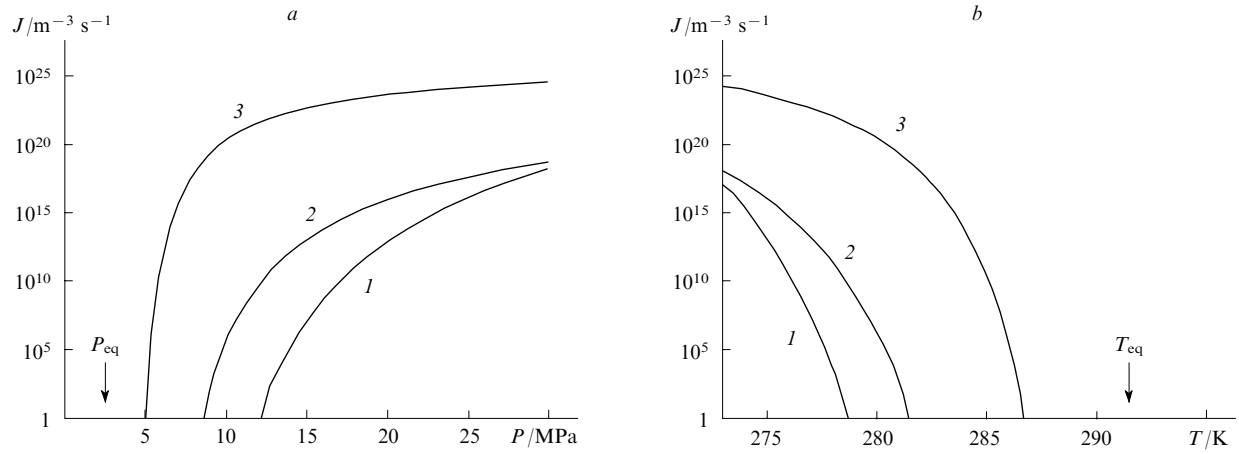


Figure 7. Methane hydrate nucleation rates in the homogeneous (*1*) and heterogeneous (*2*, *3*) nucleation at $T = 273.2$ K and various pressures (*a*) and at $P = 19.4$ MPa and various temperatures (*b*).[47]
$\theta = 90°$ (*2*) and $60°$ (*3*).

It is worth noting that these expressions are applicable to both homogeneous and heterogeneous nucleations, although the constants are different in these cases.

The calculated [47] temperature and pressure dependences of the rate of homogeneous and heterogeneous nucleation of methane hydrate for the nucleus shaped like a spherical segment are shown in Fig. 7. The calculations were carried out by Eqn (7) for isothermal conditions and by Eqn (8) for isobaric conditions. It can be seen that in both cases, the rate is higher for heterogeneous nucleation than for homogeneous nucleation. There are threshold values for the pressure elevation above the equilibrium value

$$\Delta P = P - P_{eq} \tag{8b}$$

and for the supercooling

$$\Delta T = T_{eq} - T \tag{8c}$$

Below these values, the nucleation rate becomes very low, that is, nucleation of the hydrate is a very rare event under these conditions. Upon the increase in ΔP (see Fig. 7 *a*) or ΔT (see Fig. 7 *b*) in a certain range, the nucleation rate increases very rapidly and, after that, it remains invariable.

The same researchers [47] proposed a model describing the effect of substances dissolved in the aqueous phase on the nucleation. It was noted that the additives can be sorbed on the surface of hydrate nuclei, thus decreasing their surface energy, or form additional nucleation sites in the liquid phase; they can also be sorbed on the active site surfaces of particles that are present in the solution and ensure the heterogeneous nucleation. It is clear that in the first two cases, the additives promote the hydrate formation, whereas in the third case, they impede the process. Note that the above analysis of nucleation is made under the assumption that all processes preceding the hydrate formation (such as gas dissolution and diffusion in the liquid phase) have been completed.

It has been noted above that the driving force for hydrate formation is the $\Delta\mu$ value, which can be calculated from Eqn (2) for isothermal processes and from Eqn (3) for isobaric processes. More complicated cases where both temperature and pressure vary have also been considered.[49] The situation is even more intricate when the hydrate is formed from a gas mixture. A calculation of the driving force for the hydrate formation from multicomponent gas mixtures has been reported.[50]

The time of existence of the metastable liquid phase, with a gas hydrate being the stable phase, depends on temperature, gas pressure, the pattern of variation of temperature and pressure with time, the presence and activity of heterogeneous nucleation sites in the liquid and so on.[1, 2, 21–23, 47, 48, 51] The time interval between the moment of transition of the liquid + hydrate-forming gas to the metastable state and the onset of nucleation is a random value, which is characterized by a distribution function depending on all factors indicated above.

Two methods are employed to investigate the nucleation in metastable liquids, and they are also applicable to the nucleation of gas hydrates. In the isobaric isothermal experiments, the liquid is brought to the metastable state as fast as possible (most often, by fast cooling) and, after that, the time interval between the moment when the system has become metastable and the onset of crystallization is measured at a constant pressure and temperature. An example of this type of study was reported by Knezic *et al.*[52] The second method is polythermal: the liquid is cooled at a constant rate and the temperature or supercooling at which crystallization starts is recorded.[53] Often both methods are applied in parallel to study the same system.[54] A rational way for representing the stochastic nature of nucleation are so-called survival curves or nucleation curves showing the proportion of samples in which the hydrate has not formed (survival curves) or has formed (nucleation curves) by a particular point in time *vs.* the supercooling time (or degree of supercooling).[55, 56] An example of experimental survival curves is shown in Fig. 8.

Often, quite a few experiments with one and the same sample are carried out while studying the nucleation. In this case, the obtained survival curve is known to refer to one and the same set of nucleation sites occurring in the system. If the sample is destroyed or considerably changes during the study, experiments are repeated using samples prepared in the same way. In this case, it is expedient to use setups with a large number of reactors.[57] The application of

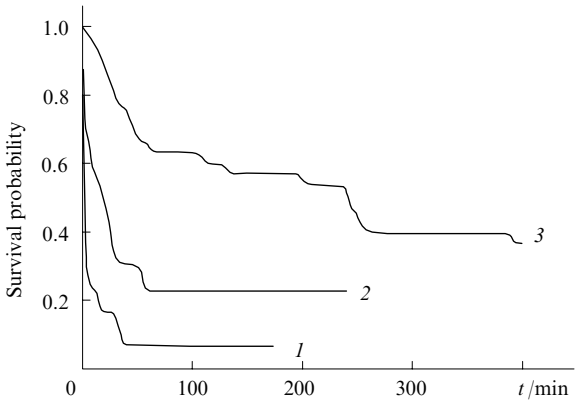


Figure 8. Survival curves describing the hydrochlorofluorocarbons hydrate formation at various temperatures.[56]
Experimental temperature /K: (*1*) 282.1, (*2*) 282.6, (*3*) 283.1

methods of this type to gas hydrate formation was started rather recently.[56–59]

The survival function obtained in an isothermal isobaric experiment is directly related to the nucleation rate inherent in a given system [60, 61]

$$\ln\frac{N}{N_0} = -Jq(t - t_0) \qquad (9)$$

where N is the number of samples in which no nuclei have been formed by time point t; N_0 is the total number of samples; t_0 is the time (s) during which the temperature reaches the specified value (dead time of the process). By q is meant the volume of the liquid in the sample for bulk nucleation, or the liquid/gas contact area for surface nucleation, or the area of heterogeneous nucleation sites present in the system.

For a sample cooled at a constant rate,[60, 62]

$$\ln\frac{N}{N_0} = \frac{q}{v}\int_{T\text{eq}}^{T} J(T)\mathrm{d}T \qquad (10)$$

where v is the cooling rate and T_{eq} is the equilibrium temperature under the experimental pressure.

II.2. Crystallization temperatures of gas hydrates (attainable degrees of supercooling)

Maeda *et al.*[58] studied the nucleation of hydrates formed by methane and a methane–propane mixture (10 mol.% of propane, structure sII) on the surface of the aqueous phase. The process was conducted in an automated high pressure reactor (HP-ALTA) with watch windows. A transparent cell with water was placed inside the reactor. The pressure was created by filling the reactor with the hydrate-forming gas, the temperature was varied according to a specified programme. The appearance of a hydrate film on the liquid phase was detected by a decrease in the transmitted light intensity. When the cooling rate was 1.5 K min^{-1}, the average supercooling for different pressures was 10–11 K, with the width of the survival curves being close to 20 K for hydrate formation and 2–3 K for ice formation. The highest hydrate nucleation temperatures were 3–6 K lower than the equilibrium temperature. An increase in the cooling rate results in a slight increase in the supercooling required for hydrate formation. Using an advanced reactor of this type, it became possible to study the effect of materials occurring in contact with liquid water on the nucleation of hydrates.[63, 64] It was found that the nucleation rate in metallic and glass containers is proportional to the length of the reactor wall/water boundary, that is, the nucleation occurs at this boundary.[63] The nucleation rate observed at the interface between water and organic liquid saturated with a hydrate-forming gas was lower and depended only slightly on the nature of the liquid.[63]

A simpler design of an automated apparatus (operating at the atmospheric pressure) was used [59] to study the nucleation of tetrahydrofuran (THF) hydrate. The THF hydrate (structure sII) is formed upon crystallization of homogeneous aqueous solutions; therefore, it is widely used as a gas hydrate model. When the THF to water molar ratio in the initial solution is 1 : 17, the resulting hydrate congruently melts at 277.5 K (Fig. 9). The study was carried out for 0.3 ml solution samples with different THF concentrations, which were placed into borosilicate glass tubes. It was found that hydrate nucleation occurs at smaller supercoolings in solutions with THF : water ratios of $< 1 : 17$ than in solutions with the 1 : 17 ratio. For a solution with 1 : 36 composition, the supercooling in the middle of the survival curve was 16.5 K, whereas for a 1 : 17 stoichiometric solution it was about 24 K. Upon the addition of a small crystal of AgI, which is a well-known ice nucleator, the supercooling required for hydrate formation reliably decreased.

Daraboina *et al.*[65] studied the formation of natural gas hydrate (88% methane) in gas–hydrocarbon–model seawater systems. Three types of crude oils, heptane and a heptane–toluene mixture served as the hydrocarbon phase. An experimental setup with five rocking cells was used, in which stirring was accomplished by stainless-steel balls placed inside the cells. In all probability, emulsions were formed in the cells. The experiments were carried out with continuous rocking of the reactors, the temperature was ramped during the experiment from 298 to 274 K, and the

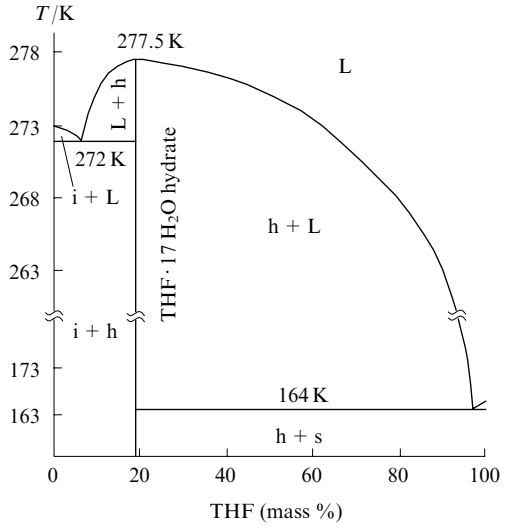


Figure 9. Phase diagram of the THF–water system.[6]
h is hydrate, L is a THF solution in water, i is ice, s is solid THF.

initial pressure was 10 MPa. The authors demonstrated that the addition of any hydrocarbon phase increases the supercooling required for the hydrate formation, this effect being enhanced with increasing concentration. Similar results have also been obtained in isothermal experiments.

Retardation of the hydrate nucleation upon the addition of heptane was also noted by Sharifi *et al.*[66] No clear correlation was found between the required supercooling and the composition of the hydrocarbon phase. It was assumed that the retardation of hydrate nucleation in the presence of hydrocarbons can be associated with the restriction of gas diffusion towards the water surface. One more possible reason is the predominant dissolution of heavy hydrocarbons in the organic phase and the concomitant change in the gas composition. Davies *et al.*[67] carried out experiments on nucleation of methane and xenon hydrates from water emulsions in crude oil using a standard differential scanning calorimeter. In both cases, the nucleation required a supercooling of ~30 K and the width of the survival curve, most often, did not exceed 2 K. As the gas pressure increased, the supercooling required for the hydrate nucleation decreased. The cooling rate (0.5–3 K min^{-1}) did not affect significantly the attained supercooling values. Stoporev *et al.*[62] determined the supercooling for the formation of methane hydrate from water emulsions in crude oil and decane. The average supercooling values were ~17 K for oil emulsions and ~20 K for decane emulsions; the width of the survival curve was ~10 K in both cases. The obtained results provided the conclusion that the attainable supercooling is affected by the system components (surfactants, heavy oil components) adsorbed at the water/organic liquid interface.

II.3. Induction time of hydrate formation

The induction time of hydrate formation is the time interval between the moment when the system becomes metastable with respect to hydrate formation and the moment when the onset of hydrate formation is detected in the system. This time interval is stochastic and has its own distribution function, which is determined by the type of nucleation, the growth rate of hydrate nuclei, the sensitivity of detection methods and so on. Therefore, the induction time is not a strict and unambiguous system characteristic; it can vary from several minutes to tens of hours.[1,2,21,22] An increase in the driving force of nucleation usually decreases the scatter of induction time values observed in experiments.

Kashchiev and Firoozabadi[48] presented a theoretical model for calculating the value determined in experiments — the most probable (average) induction time of hydrate formation (t_i). In that study, it was assumed that t_i corresponds to the moment when the degree of conversion of reactants to the hydrate is 1% and it becomes possible to observe the hydrate phase in the system. The authors considered two types of nucleation:

— progressive nucleation in which the formation of new nuclei capable of spontaneous growth and the growth of hydrate particles that have appeared earlier proceed in parallel;

— instantaneous nucleation in which all nuclei are formed in the system over a short period of time and subsequently only growth of the hydrate particles takes place.

In the study cited, the mathematical description of the growth of nuclei assumes that the growth rate does not depend on the particle size and is a power function of time. Equations were derived describing the dependence of the induction time on the system parameters. In the case of isothermal conditions of hydrate formation:

for instantaneous nucleation,

$$t_i = K(S-1)^{-1} \tag{11}$$

for progressive nucleation,

$$t_i = K\left[S(S-1)^{3m}\right]^{-1/(1+3m)} \exp\left(\frac{B}{(1+3m)(\ln S)^2}\right) \tag{11a}$$

where S is calculated in the same way as in Eqn (7a).

In the case of isobaric conditions,

for instantaneous nucleation,

$$t_i = K\left[\exp\left(\frac{\Delta S_e \Delta T}{kT}\right) - 1\right]^{-1} \tag{12}$$

for progressive nucleation,

$$t_i = K\exp\left(-\frac{\Delta S_e \Delta T}{kT}\right) \times \tag{12a}$$

$$\times \left[1 - \exp\left(-\frac{\Delta S_e \Delta T}{kT}\right)\right]^{-3m/(1+3m)} \exp\left(\frac{B'}{(1+3m)T\Delta T^2}\right)$$

In Eqns (11)–(12a), K, B, B' are constants, m is the exponent in the power law describing the growth of the hydrate particles (varies from 0.5 to 1).

The calculated pressure and temperature dependences of the induction times for progressive nucleation of the methane hydrate for homogeneous and heterogeneous nucleation cases are presented in Fig. 10. It can be seen that the induction time rapidly changes with variation of the temperature and pressure. For the cyclopropane–water system, a good agreement was shown between the predicted and experimental values for the induction time.[48] Sarshar *et al.*[68] used a similar approach to calculate the induction times of hydrate formation for a hydrocarbon mixture. A good correlation between the values determined by this method and observed in experimental formation of propane hydrate has been noted in another study.[69]

Wu *et al.*[70] investigated the dependence of the induction time of formation of binary methane and propane hydrate on the pressure and temperature. The above-mentioned HP-ALTA apparatus was used. At a pressure of 4.3 MPa and supercooling of 6 K, the hydrate formation over a period of 200 min was observed only in 60% of experiments, whereas at 11 K supercooling and the same pressure, hydrates were formed within < 10 min in all experiments. It may happen that a hydrate which is metastable under the experimental conditions is the first to be nucleated. For gas mixtures, this possibility has been demonstrated.[71,72] Sun *et al.*[73] studied in detail the nucleation time distribution for THF hydrate as a function of supercooling and composition of the system. It was shown experimentally that the nucleation time distribution obeys a log-normal law. It was found that the induction time and the distribution width decrease with increasing degree of supercooling of the system, upon the addition of solid particles (quartz sand) and in the presence of dissolved ions in the aqueous phase. The increase in the supercooling from ~8 to ~13 K resulted

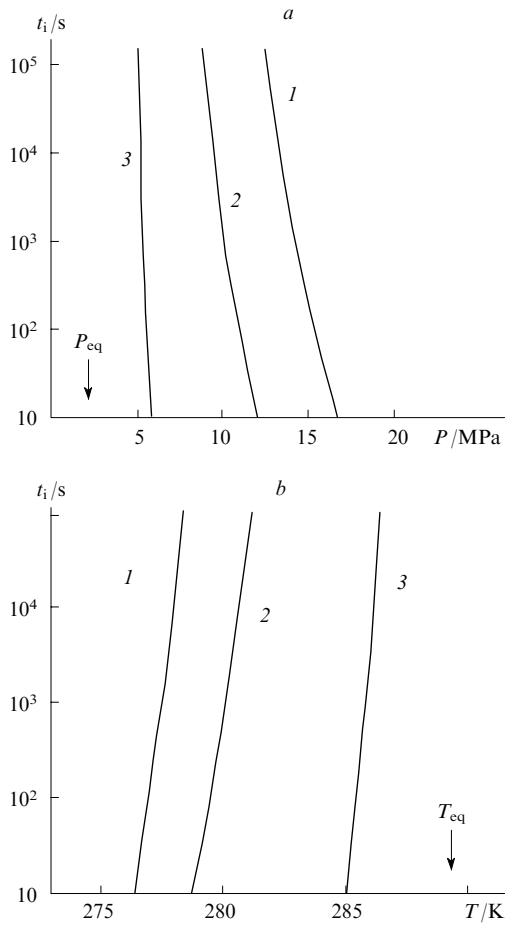


Figure 10. Induction times of methane hydrate formation at various pressures [T = 273.2 K, Eqn (11a)] and temperatures [P = 19.4 MPa, Eqn (12a)] for homogeneous (*1*) and heterogeneous (*2*, *3*) nucleation calculated in Ref. 48.
$\theta = 90^\circ$ (*2*) and 60° (*3*).

in shortening of the induction time by 1–2 orders of magnitude.

To summarize the above, it can be stated that the bottleneck of many studies is the lack of information about the particular nucleation site of the hydrate. It is beyond doubt that virtually in all cases, researchers were dealing with heterogeneous nucleation. The experimental setups used in various studies were made of different materials and had different (most often, unknown) state of the surfaces (oxidized; containing adsorbed foreign substances and so on). All this hampers comparison of the results of investigations. More complications are created by the unknown background of microparticles present in the aqueous phase and capable of acting as heterogeneous nucleation sites. Some of the authors cited above (*e.g.* Refs 59, 63 and 64) made attempts to solve these problems; however, study of the activities of various surfaces as gas hydrate nucleation sites is still a topical research issue.

II.4. Effect of the surfaces inserted into the aqueous phase on the nucleation of hydrates

Currently, the methods for accelerating the nucleation of hydrates by adding various powders to water (often in the presence of surfactants) are the subject of vigorous research. If sticking of the hydrate nucleus to a solid surface of a powder particle reduces the surface energy of the hydrate, this particle increases the nucleation rate and, hence, decreases the induction time of hydrate formation or attainable supercooling. However, if the foreign surface can deactivate the active sites of nucleation present in the aqueous phase (*e.g.*, by adsorption), the hydrate nucleation rate can decrease. Investigations of this type are important for the search for catalysts of hydrate formation which could be added to the aqueous phase to implement the hydrate formation process with a much shorter induction time. Also, of great interest are the chemical composition and structure of surfaces that facilitate or hamper the hydrate formation. This information has been virtually absent until recently.

A statistical study of the induction time of CO_2 hydrate formation in aqueous suspensions of montmorillonite clay and sea bottom sediments has been reported.[57] The thermodynamic supersaturation was created in the system by rising pressure at a maximum possible rate and, after that, the time variation of the sample temperature was recorded. The onset of hydrate formation was detected by the abrupt change in temperature and by sight. The experiments were carried out at a pressure of 2–3 MPa and a temperature of 273.5–275 K. The observed distribution of induction times is described satisfactorily by a log-normal law. Like in the study cited above,[73] the distribution maximum shifted towards shorter times with increasing thermodynamic supersaturation (temperature decrease and pressure rise, Fig. 11). The induction times for suspensions were shorter than for pure water and were markedly different from one another. For the suspension of montmorillonite clay in pure water, the distribution maximum occurred at t = 30 min; for suspensions of the same clay in a 3.5% NaCl solution, the maximum was at t = 18 min; and for suspensions of the sea sediment in water, it was at t = 12 min. Thus, the added materials used in these experiments catalyzed the hydrate formation. The high activity of the bottom sediment was attributed to the presence of a large amount of organic compounds in this material.

Experiments of similar design dealing with the induction times of THF hydrate formation were carried out by Dai *et al.*[74] They found that at a supercooling of 7.5 K, the distribution maximum of the induction times of freezing of the $THF \cdot 17\,H_2O$ stoichiometric solution (below referred to as 1 : 17 composition) amounted to ~14 min, and the position of the maximum virtually did not change upon the addition of chemically pure precipitated calcium carbonate. Upon the addition of kaolinite, silts or pulverized natural calcite, the distribution maximum shifted by 1–3 min. In addition, it was shown that the induction time somewhat decreased upon severe mechanical impact on the solution.

It has been shown[75] that glass particles with hydrophobized surface can substantially accelerate the nucleation of methane, THF and cyclopropane hydrates. Whereas without additives nucleation did not occur in any of the systems over a period of 12 h, in the presence of hydrophobized powders (and in some cases, also untreated glass powder), nucleation was observed in 50%–100% of experiments. The addition of one and the same powder to the aqueous phase affects hydrate formation by different substances in different ways. Wang *et al.*[76] studied the nucleation of methane hydrate on the surface of quartz modified

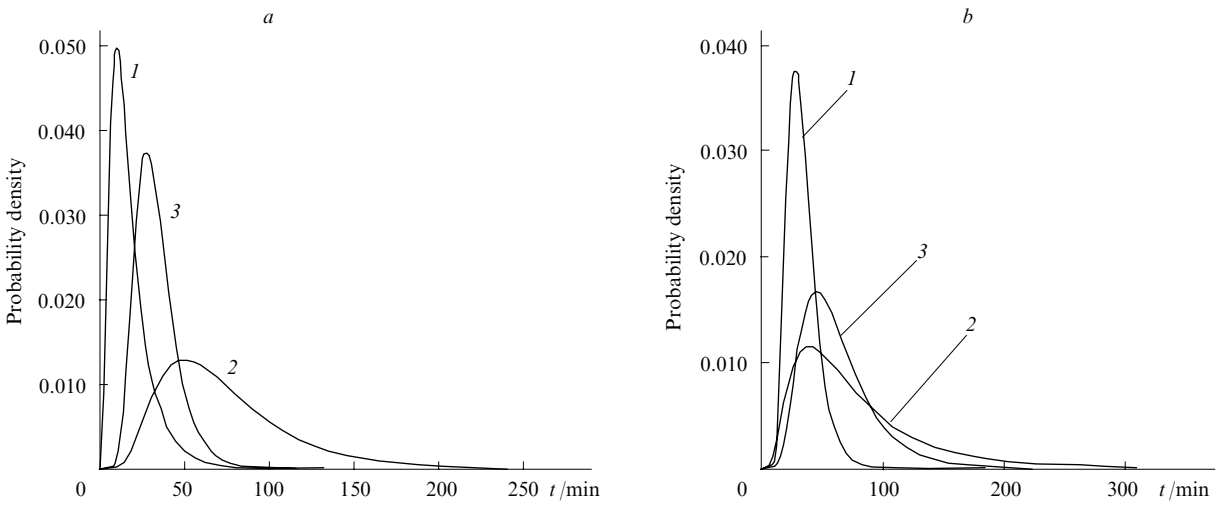


Figure 11. Effect of pressure (*a*) and temperature (*b*) on the distribution of the induction times of CO_2 hydrate formation from a suspension of montmorillonite clay in a 3.5% NaCl solution. Drawn on the basis of Ref 57.
(*a*) T = 273.5 K; P = 3.0 (*1*), 2.5 (*2*), 2.2 MPa (*3*); (*b*) P = 3.5 MPa; T = 273.5 (*1*), 274.2 (*2*), 274.7 K (*3*).

with octadecyltrichlorosilane. It was shown that the induction time of methane hydrate formation in the presence of hydrophobized powders rapidly decreased with increasing water contact angle of the powder surface. According to the data of Zhou *et al.*,[77] upon the addition of graphite nanopowder to water, the induction time of CO_2 hydrate formation decreased from 47 to 8 min at 2.5 MPa pressure (supercooling of ~4 K) and from 20 to 3.5 min at 6.5 MPa pressure (supercooling of 6 K), and furthermore the growth of the hydrate particles accelerated. It has been noted [78] that for supercooling of ~16 K, the induction time of ethylene hydrate formation decreased more than 20-fold in the presence of graphene oxide compared with the hydrate formation in pure water. Under experimental conditions used in the cited work, graphene oxide accelerated the nucleation of the hydrate more efficiently than sodium dodecyl sulfate. Finally, it has been shown [79] that the influence of nanoparticles suspended in water on the induction time of hydrate formation is related to the chemical composition of their surface rather than to the material that forms the particles. A correlation was found between the observed induction times of hydrate formation and the content of carbon on the particle surface.

To date, a series of studies have been performed dealing with the nucleation and growth of hydrates from surfactant-stabilized suspensions of metal or metal oxide nanopowders in water. A synergistic effect of several additives in the aqueous phase has been demonstrated.[80] The addition of small concentrations of sodium dodecyl sulfate or silver nanoparticles into water did not have a noticeable effect on the induction time of hydrate formation, whereas these substances added together to the aqueous phase decreased the induction time. Unfortunately, the induction times observed in this study were short; therefore, the conclusion about the synergistic effect of these additives is not quite reliable. More pronounced differences were found in other studies.[81–83] Najibi *et al.*[81] investigated the formation of methane hydrate with the simultaneous presence of copper oxide powder and sodium dodecyl sulfate; the supercooling was ~5 K. In all cases, when both copper oxide powder and sodium dodecyl sulfate were present in the aqueous phase, the induction time decreased 1.5 – 5-fold; an increase in the content of copper oxide resulted in shortening of the induction time. The addition of the surfactant alone was less efficient. Pahlavanzadeh *et al.*[82] studied the formation of methane hydrate in the presence of copper nanopowder and cetyltrimethylammonium bromide as the surfactant at the same supercooling. In the presence of copper powder, the induction time decreased ~3-fold with respect to that in pure water; the presence of the surfactant or both the nanopowder and the surfactant had a less pronounced effect. Finally, a study [83] has addressed the effect of zinc and aluminium oxides in the presence of sodium dodecyl sulfate on the formation of sII hydrate from a hydrocarbon mixture. At a supercooling of 8 K and the simultaneous presence of oxide particles and sodium dodecyl sulfate, the induction time of the hydrate formation decreased 2 – 3-fold compared with the induction time found for pure water; the presence of the surfactant alone was less efficient. In all of the above cases, the presence of the solid particles, the surfactant or both increased the degree of conversion of water to the hydrate and accelerated the growth of hydrate particles.

Thus, it can be concluded that metal surfaces and hydrophobic-hydrophilic surfaces (oxidized organic surfaces, oxide surfaces partly coated by hydrophobic groups, *etc.*) are the most probable candidate catalysts for the hydrate nucleation. Presumably, some sites of the hydrophobic-hydrophilic surfaces are complementary to the hydrate surface and are able to accommodate the hydrophobic moieties in the open cavities located on the hydrate surface, while the hydrophilic sites can bound the hydroxyl groups located on the hydrate surface.

II.5. Hydrate formation and water memory

The experience in the field of gas hydrates attests to the possible existence of so-called water memory effect, which is manifested as a dependence of the induction time of hydrate formation on the liquid phase prehistory. Indeed, the induction time of hydrate formation was substantially

shorter for water formed upon ice melting or hydrate decomposition than for freshly distilled water.[1,2,80] It has been shown[22] that the induction times of propane hydrate formation for water after several hydrate formation–dissociation cycles are of the order of one hour and are reproduced to within 20%, whereas for 'unprepared' water this time period varies from several hours to tens of hours. Among recent publications that support the existence of this effect, studies of Ohmura *et al.*[56] and Wu *et al.*[84] deserve mention. It is noteworthy that some publications dispute the existence of the memory effect. Indeed, this effect was not detected in the freeze–thaw cycles of the THF hydrate.[85] In methane hydrate formation–dissociation cycles repeated many times, the induction times were similar in the first and last cycles.[86] In the researchers' opinion, this attests to the absence of memory effect. However, analysis of numerous published data indicates that the water memory effect still does exist, although it may not always be observed. It is worth mentioning that we observed this effect in some experiments.

The mechanism of this phenomenon at the molecular level is not clear as yet. The following main hypotheses proposed to explain the memory effect have been considered in detail:[26]

— retention of some fragments of hydrate structure in the liquid water, the presence of which facilitates the repeated hydrate formation;

— formation of a supersaturated gas solution in water as a result of hydrate dissociation; this increases the driving force of hydrate formation and facilitates the hydrate nucleation;

— formation of molecular imprints of the hydrate crystals on the surfaces present in the system, which subsequently act as the nucleation sites for hydrates.

Recent studies add some interesting details to the memory effect issue. It was found[87] that liquid water formed after hydrate dissociation contains micro- and nano-sized gas bubbles, which can exist for 24 h. The authors attributed the memory effect observed in experiments to the presence of these bubbles. The memory effect was manifested in different ways in different experimental cells.[88] Furthermore, it was convincingly demonstrated that the effect is mitigated with increasing solution overheating upon decomposition of the hydrate. Similar observations were described in earlier publications; however, Sowa and Maeda[88] were the first to substantiate this by collecting sufficient statistics. It is noteworthy that for equal driving forces of the process, the induction time of hydrate formation is minimized when the temperature of the aqueous phase is close to the melting point of ice, while at temperatures of 275–278 K, it increases severalfold.[22] Probably, this can be attributed to the known fast hydrate formation upon thawing of ice in the hydrate-forming gas atmosphere at a sufficient gas pressure.[1,2] It cannot be ruled out that the mechanism of this phenomenon resembles the mechanism of memory effect in the hydrate formation.

III. Growth and dissociation of gas hydrates

After nucleation of gas hydrate, the system (reactor) contains hydrate particles, liquid water (or ice) and the hydrate-forming component. Further growth of the hydrate particles is determined by heat and mass transfer processes taking place in the system and by the kinetic characteristics of hydrate formation. The heat and mass transfer rates depend on the system geometry, the presence (and intensity) of stirring, the rate of heat withdrawal and morphology of growth of hydrate particles.[1,2] Thus, to describe the kinetics of hydrate growth, it is necessary, first, to identify the rate-limiting step and, second, to construct a mathematical model describing the amount of hydrate formed as a function of time. The rate constants for proper hydrate formation reactions, that is, characteristics of the intrinsic kinetics of the process, are usually unknown parameters in the kinetic models of hydrate formation. These parameters are most demanded and are used, for example, in the engineering design of reactors meant for the formation of hydrates. The processes of hydrate dissociation at temperatures above and below 273 K are qualitatively different; therefore, in what follows they are considered separately.

The number of moles of consumed gas, which is an easily measurable value, is used most often in the kinetic measurements of hydrate growth to characterize the degree of transformation. The following situations have been studied in most detail:

— the hydrate is formed as the mixture is vigorously stirred in the reactor with excess water and in the presence of a gas phase with a constant pressure;

— the hydrate is formed without stirring.

A detailed review of the kinetic studies of the hydrate growth has been published.[23,89] Most often, the growth (dissociation) rate is evaluated from the change in the amount of the gas in the gas phase per unit time

$$\frac{\mathrm{d}n_\mathrm{h}}{\mathrm{d}t} = KA_\mathrm{p}(q - q_\mathrm{eq}) \qquad (13)$$

where $\mathrm{d}n_\mathrm{h}/\mathrm{d}t$ is the growth (dissociation) rate of the hydrate, *i.e.*, the number of the gas moles consumed during hydrate growth or released upon hydrate dissociation per unit time/s^{-1}; K is the rate constant (a negative value for dissociation); A_p is the surface area of the hydrate/m^2; $(q-q_\mathrm{eq})$ is the driving force, which can be represented by substantially different characteristics of the process in various models. In the simplest case where neither the driving force nor the hydrate surface area change, solving this equation gives a linear dependence of n_h on t, that is, the hydrate growth (dissociation) rate does not vary with time. However, most often, the surface area and the driving force do not remain invariable during the process; therefore, the kinetic equation becomes more intricate.

Lately, some kinetic data about displacement of the guest molecule in the hydrate have been reported. The displacement of methane in the hydrate by carbon dioxide has been studied.[90,91] These studies are aimed at both the development of scientific grounds of methane production from hydrate accumulations and sequestration of carbon dioxide. The displacement was shown to occur very slowly and to accelerate as the pressure, temperature and CO_2 concentration increase. Indeed, at $\sim$273 K, methane hydrate powder reacts with carbon dioxide gas, resulting in 30% replacement of CH_4 by CO_2 in the hydrate phase within six days. Similar values were found for liquid CO_2. Falenty *et al.*[92] performed an integrated study of methane replacement in the hydrates by CO_2 using low-temperature electron microscopy, powder neutron diffraction and Raman spectroscopy. The process was found to comprise two stages: first, fast exchange of molecules in the surface

layer and, second, slow double-sided exchange of molecules between the hydrate central region and the surrounding gas mixture. The exchange mechanism of guest molecules was discussed considering the obtained results. A program package for modelling the gas exchange under real geological conditions has been developed.[93] The results of calculations were compared with the results of experiments on a laboratory setup.

III.1. Growth of gas hydrates in the systems with liquid water and gas without stirring

The morphology of gas hydrates formed under various conditions is fairly diverse. A more or less dense hydrate film appears at the stationary interface between liquid water and a gas, as a rule, *via* sticking together of crystals formed on the surface. The growth of this film on the liquid surface can occur at a considerable rate — 0.05–0.7 m s^{-1}; the film thickness in the case of gases poorly soluble in water (methane) is ~0.1–0.01 mm, while for readily soluble gases (carbon dioxide), the film thickness is slightly less than 1 mm.[94–99] The film thickness is inversely proportional to the driving force of the process.[100] The morphology of the hydrate film growth front can considerably differ for small (<2 K) and large supercoolings.[101] For small supercooling, the growing surface front was a broken line (apparently, the surface was composed of faces of a small number of crystallites), while in the case of large supercooling, the film consisted of small crystallites and the growth front was a curve. The hydrate film growth at the water/liquid hydrocarbon interface did not differ qualitatively from the growth at the gas/water contact.[102] Analysis of their own and published data carried out by Imasato *et al.*[102] demonstrated that the growth rate of the hydrate film increases with increasing supercooling.

After hydrate formation on a free liquid surface, further growth occurs along the normal to the interface, mainly towards the aqueous phase. Initially, the rate of this process is 1–2 orders of magnitude lower than the propagation rate of the hydrate film across the gas/liquid interface; as film thickness increases, the hydrate formation rate decreases down to complete termination. The dependence of the lateral (across the gas/water interface) rate of the growth of hydrate films on the driving force is close to exponential.[100, 103] It was concluded [100, 104] that the growth rate of such films is controlled by heat withdrawal, and kinetic models of the processes were proposed. For the supercoolings of >3 K, the growing hydrate film consists of needle-like and triangular crystallites; at lower supercooling, the hydrate crystals grow on the surface as large polygons with sides up to 1 mm.[105] A study of the morphology of a hydrate film growing on the liquid surface as a function of pressure demonstrated [86] that the film formed at $P \approx 16$ MPa is less dense than the film formed at $P = 7–10$ MPa.

III.2. Growth of gas hydrates in stirred systems with liquid water and gas

When the aqueous phase is vigorously stirred, the hydrate film on the water surface is destroyed and the hydrate crystals and their aggregates that have formed are spread throughout the aqueous phase in which they grow. The process of hydrate growth includes several stages: dissolution of gas components in the aqueous phase, their transport towards the hydrate particle, hydrate formation reaction in the 'transient layer' adjoining the particle, and withdrawal of heat formed in the reaction. Note that in this Section, we mainly consider cases with vigorous stirring of the aqueous phase in which the velocity of stirring does not affect the observed process rate, *i.e.*, the concentration of the dissolved gas is constant throughout the solution. The setup used in these experiments is, most often, a temperature-controlled reactor with a stirrer and a gas-dosing system. The constant pressure in the reactor is maintained *via* gas delivery, the amount of the delivered gas being equal to the amount of gas that is consumed *via* reaction (or is dissolved in the liquid). The reactors for kinetic experiments can be additionally equipped with devices for determination of the size and concentration of the hydrate particles formed in the liquid.

A typical dependence describing the change in the amount of consumed gas for a kinetic experiment on hydrate formation and dissociation carried out in a reactor of this type is presented in Fig. 12. In the initial stage (segment 0–*1*), gas saturation of the aqueous phase takes place; during this period, the gas pressure in the reactor is maintained constant, being higher than the equilibrium pressure of hydrate formation at the experimental temperature. Analysis of the shape of this curve segment can be used to determine the kinetic characteristics of gas dissolution in water. At the point of time designated by *1*, hydrate nucleation takes place; this is followed by the growth of hydrate particles, and, therefore, the amount of the absorbed gas sharply increases. Segment *1–2* corresponds to the kinetic curves of gas absorption, analysis of which in terms of the models considered below provides kinetic characteristics of the hydrate growth. The gas pressure and temperature in the reactor are maintained the same in this stage as in the previous stage. If the experiment protocol envisages dissociation of the hydrate, then the pressure is lowered down to a value somewhat exceeding the equilibrium pressure; for stabilization, the system is kept under these conditions for some period of time (segment *2–3*). Subsequently (time point *3*), a pressure below the equilibrium one is established and dissociation of the hydrate takes place (segment *3–4*). Analysis of the kinetic curves in the final segment can be used to determine the kinetic parameters of hydrate dissociation. The choice of the driving force for the formation and dissociation processes

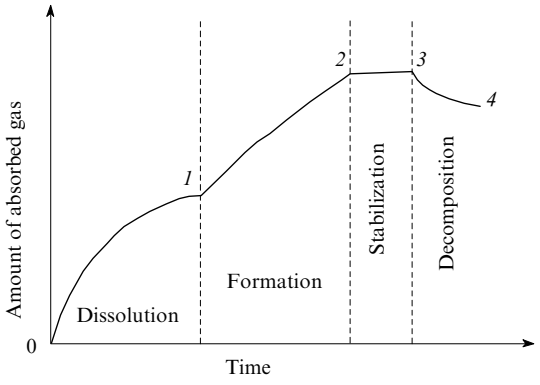


Figure 12. Typical time dependence of the amount of absorbed gas in kinetic experiments.
(*1–4*) see text.

in the kinetic equation (13) is dictated by the model used. The hydrate/liquid interfacial area is calculated from the hydrate particle size distribution, which can be either calculated or measured experimentally.

There are a number of kinetic models describing the formation and dissociation of hydrates in these systems. An early model known as the EKDB model,‡ was proposed by Englezos *et al.*[106] According to this model, the growth of hydrate particles in the reactor includes the following stages:

— dissolution of the hydrate-forming gas in the liquid;

— gas diffusion in the liquid towards the growing hydrate particle;

— growth of the hydrate particle.

The difference between the fugacities of the gas dissolved in water under experimental conditions (f) and the gas in equilibrium with the hydrate and the liquid phase (f_{eq}) was taken as the driving force of the process. By analogy with Eqn (13), the hydrate growth rate was written in the form

$$\left(\frac{dn_h}{dt}\right)_{P=\text{const}} = KA_p(f - f_{eq}) \qquad (14)$$

where $1/K = 1/k_r + 1/k_d$, k_r and k_d are the rate constants for hydrate formation and for hydrate-forming gas diffusion towards the hydrate particle, respectively.

Owing to vigorous stirring, the $1/k_d$ value is assumed to be negligibly low and the concentration of the hydrate-forming gas in water is taken to be invariable. The heat and mass transfer issues are not considered in this model, as it is assumed that stirring ensures an efficient withdrawal of heat released during the hydrate formation reaction. The growing hydrate particles are distributed over the whole volume of the liquid phase. According to this model, it is generally assumed that the concentration of the hydrate-forming gas dissolved in the liquid is a result of two simultaneous processes — transfer of the hydrate-forming gas through the surface layer of the liquid (actually gas dissolution) and consumption of the dissolved gas in the hydrate formation reaction. In a steady-state process, the concentration of the dissolved gas is constant. The rate of dissolution can be determined in special experiments.

In early studies in which the experimental data were treated in terms of the EKDB model, the surface area of hydrate particles was calculated on the basis of the nucleation theory with the assumption of instantaneous nucleation of all hydrate particles. This brought about substantial errors in determination of the number of hydrate particles and particle size distribution. In a later study,[107] data on the number of hydrate particles in the reactor and particle size distribution were obtained by focused beam reflectance measurements. The key result derived from the experimental data is the determination of the rate constant of hydrate formation k_r and its temperature and pressure dependences. The EKDB model was invoked for treating experimental data and calculating the rate constants for the formation of CO_2 hydrate,[107] methane and ethane hydrate[108] and hydrates of propane and propane–ethane mixture.[109] A method for calculation of the rates of hydrate formation from gas mixtures using this model has been proposed.[110]

Numerous attempts have been made to improve the kinetic model. Several developed models have been surveyed in detail in a review.[23] We will consider some of them. The excess of concentration of dissolved gas over the equilibrium concentration in the presence of the hydrate was proposed as the driving force for the hydrate formation process.[111] In this model, the pressure is taken to be invariable throughout the system. The hydrate particles grow in such a way (Fig. 13) that the temperature on the particle surface ($T_{h/L}$) is somewhat higher than the temperature of the liquid (T_L), because of the heat evolved in the reaction, and the surface concentration of the hydrate-forming gas ($x_{h/L}$) is equal to its concentration in the aqueous solution equilibrated with the hydrate at the given temperature and pressure. In the thin transient layer adjoining the hydrate particle surface, the concentration of the hydrate-forming gas increases and the temperature decreases to reach the values characteristic of the bulk liquid phase (x_L and T_L, respectively). In the bulk liquid phase, these values are constant owing to stirring. The concentration of the hydrate-forming gas in the liquid phase is determined by the difference between the rates of gas dissolution in water and the methane hydrate formation. Finally, a transient layer appears again at the gas/liquid interface, in which the concentration of dissolved hydrate-forming gas increases from the value characteristic of bulk water during the hydrate formation to the equilibrium concentration of a saturated solution of the hydrate-forming gas in water ($x_{g/L}$) in the absence of the hydrate (for the given temperature and pressure). The temperature in this layer also changes. Relying on this model and using the approach proposed previously,[106] Bergeron and Servio[112] created a new kinetic model and applied it for analysis of experimental results on the growth kinetics of various hydrates. The kinetic equation for the reaction in this model is

$$\left(\frac{dn_h}{dt}\right)_{P=\text{const}} = \frac{C_{w_0}(x_{g/L} - x_{h/L})}{(A_h k_r)^{-1} + (k_{g/L} A_{g/L})^{-1}} \qquad (15)$$

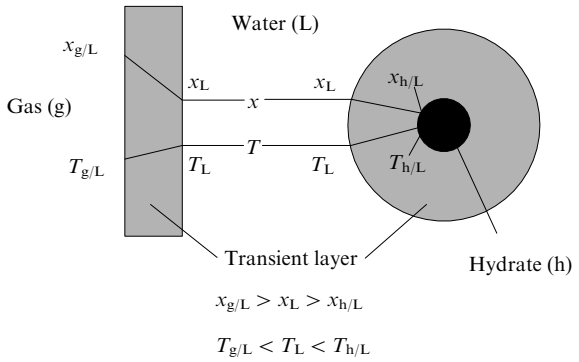


Figure 13. Variation of the temperature and concentration (x, mole fraction) of the gas in the liquid phase at gas/liquid (g/L) and hydrate/liquid (h/L) interfaces in the kinetic model proposed in Refs 111 and 112.
Pressure is assumed to be constant throughout the volume.

‡ This name is composed of the first letters of the names of the authors: Englezos – Kalogerakis – Dholabhai – Bishnoi.

where C_{w0} is the initial concentration of water in the reactor (constant), $x_{g/L}$ and $x_{h/L}$ are the mole fractions of dissolved hydrate-forming gas at the gas/liquid and hydrate/liquid interfaces, respectively; A_h is the surface area of the hydrate particle, $A_{g/L}$ is the gas/liquid interfacial surface area, k_r and $k_{g/L}$ are the rate constants of hydrate formation and mass transfer in the gas/liquid surface layer. The rate of mass transfer in the layer adjoining the hydrate particles was considered to be high and was not taken into account in the calculations.

The presented model was further developed by the same researchers.[113,114] It was shown experimentally[114] that the concentration of the hydrate-forming gas dissolved in the liquid bulk does not change during hydrate formation. This allowed the authors to avoid consideration of the stage of diffusion of the hydrate-forming gas through the liquid/gas interface (the authors assumed that particularly this stage introduces the error into the kinetic model due to the neglected influence of the solid particles present in the liquid on the gas/liquid mass transfer, *i.e.*, actually on the rate of gas dissolution in water). The study showed that the kinetic constants of the growth of hydrates of various gases considerably differ from one another. For example, the rate constants of methane hydrate growth were 8.3×10^{-8} m s^{-1} at 275.1 K and 61.5×10^{-8} m s^{-1} at 279.1 K;[115] those for CO_2 hydrate were 1.8×10^{-8} m s^{-1} at 275.5 K and 18.0×10^{-8} m s^{-1} at 279.1 K;[113] finally, for propane hydrate, the rate constant was found to be 22×10^{-8} m s^{-1} at 274 K.[112] More recently,[116] the proposed model was used to analyze the formation of the binary ionic clathrate hydrate of tetrabutylammonium bromide and CO_2.

Apart from the models considered above, quite a few models provide satisfactory description for gas absorption curves and the trends observed in experiments. According to the model proposed by Skovborg and Rasmussen,[117] the only stage limiting the rate of hydrate formation is the gas diffusion from the surface to the liquid bulk (non-stirred system). A fairly intricate model that considers simultaneously the growth and nucleation of hydrate particles was proposed by Herri *et al.*[118] According to this model, the reaction mixture is assumed to consist of two zones, a thin zone near the gas/liquid interface, in which only primary nucleation (*i.e.*, the nucleation that does not involve destruction of existing or origination of new particles on the surface of existing particles) takes place as a result of high supersaturation, and the bulk zone, in which both the nucleation and growth of the hydrate take place. The model takes into account the possibility of secondary nucleation of the hydrate within the liquid bulk *via* destruction of already existing hydrate particles. The model construction and calculations made use of the experimentally determined rate of gas dissolution in the liquid and the number and size of hydrate particles found by turbidimetry.

The kinetics of methane hydrate formation in the stirred reactor was satisfactorily described[119] in terms of a model in which heat transfer was the rate-limiting stage. It was assumed that the temperature within the stirred liquid is constant and the heat released upon hydrate formation is spent for heating of the reaction medium and is withdrawn through the reaction walls.

The models considered above have been developed for a reactor in which the hydrate particles grow in a liquid layer that is vigorously stirred (stirred reactor). Other types of reactors will be considered briefly. A mathematical model for the operation of a reactor in which water is sprayed into the compressed gas has been constructed and some data obtained experimentally for this type of apparatus have been reported.[120] The mathematical description of hydrate nucleation and growth was based on models proposed by Kashchiev and Firoozabadi.[47–49] A surfactant was added to accelerate the hydrate formation (see below). A study[121] is devoted to the induction time of hydrate formation and the rates of growth of the lower hydrocarbon and CO_2 hydrates in a gas/liquid flow. The researchers used a laboratory 'loop' — an apparatus for simulation of pipeline processes; water and aqueous solutions of kinetic hydrate inhibitors (which are considered in more detail below) served as the liquid phase. The nucleation and hydrate growth models[47–49] were used to develop a mathematical model describing the rate of hydrate formation in the system. The parameters calculated according to this model were in good agreement with experimental results. Kendoush *et al.*[122] studied the formation of the hydrate from refrigerant R12 in a water-filled column maintained at a constant temperature, with boiling R12 being supplied into the column as drops. The formation of binary THF and methane hydrate was studied in a bubble column filled with an aqueous solution of THF, with methane being bubbled through the column.[123] A similar type of reactor has been used[124] to investigate the formation of CO_2 hydrate: mass transfer in the presence of a substantial amount of hydrate suspension in the liquid phase was considered. Hydrates were also formed by spraying water onto a cooled surface by means of a compressed gas.[125] A flow type reactor was used[126] to form the CO_2 hydrate in a multiphase flow. A study of the rate of formation of binary cyclopentane and methane hydrate in a vigorously stirred reactor demonstrated[127] that the process rate is limited by methane diffusion through the reaction medium.

A detailed experimental study of the factors affecting the rate of hydrate formation in a stirred reactor has been reported.[128] Apart from the degree of supercooling and stirring rate, the researchers considered the effect of the total amount of water in the reactor and the reactor size. Interestingly, a decrease in the amount of water, all other factors being the same, accelerated the hydrate formation. The authors attributed this to a change in the hydrodynamic stirring conditions. For hydrocarbon mixtures that form sII hydrates, it has been shown[129] that the higher the concentration of heavy components in the gas mixture, the higher the growth rate and the degree of water conversion to the hydrate. This trend was interpreted as being due to the increase in the concentration of building units corresponding to large cavites with increasing content of heavy hydrocarbons. Lee *et al.*[130] investigated the formation kinetics of sH hydrates of *tert*-butyl methyl ether, methylcyclohexane and neohexane with methane being used as the help component. The process was conducted in a stirred reactor, which was charged with water and the hydrate-forming gas, and gas pressure was created. Two key parameters were measured: the induction time of hydrate formation and the hydrate formation rate in the initial period. As the driving force of the reaction, the authors considered the pressure excess over the equilibrium pressure. The resulting values were obviously stochastic; however, some trends were clearly distinguished. First of all, water solubility of liquid hydrate-forming gases decreases in the following order:

tert-butyl methyl ether > neohexane > methylcyclohexane

The rate of hydrate formation in the early stage of the process decreases in the same order. The induction times clearly tend to increase in this sequence; in addition (as expected), they increase with decreasing driving force of the process. The absolute values of the induction times varied from several or several tens of minutes to several thousands of minutes; at low driving forces ($\leqslant 1$ MPa), methylcyclohexane and neohexane hydrates did not form, in some cases, for 5 days.

Generally, the successful use of a number of markedly different models for describing the hydrate formation in a stirred reactor indicates that the process kinetics depends, most likely, on all of the listed factors — the intrinsic kinetics and heat and mass transfer. In most cases, the intrinsic kinetics of hydrate formation can hardly be the rate-limiting stage and the obtained results are extremely sensitive to the design of experimental equipment and to specific features of the system involved. In conclusion of this Section, note that in the last decade, exploratory research has been carried out for the design of mechanical carriers for liquid water meant for increasing the gas/water contact area and, hence, providing high hydrate formation rate. This subject matter has been surveyed by Linga and Clarke.[131]

III.3. Dissociation of gas hydrates in systems of liquid water and gas

Approaches resembling those considered above have been used to construct a mathematical model for hydrate dissociation and to process experimental data.[132–135] It was assumed that during dissociation, a hydrate particle is surrounded by a thin layer of released gas. The dissociation rate is determined by three factors: the intrinsic dissociation reaction rate, the rate of product escape to the bulk (bubble detachment and gas dissolution in water) and the rate of heat supply to the hydrate particle. The authors assumed that the second and third factors can be considerably suppressed by vigorous stirring of the content of the reactor. The kinetic equation has the form

$$\left(\frac{\mathrm{d}n_\mathrm{h}}{\mathrm{d}t}\right) = -KA_\mathrm{p}(q_\mathrm{eq} - q) \qquad (16)$$

where $\mathrm{d}n_\mathrm{h}/\mathrm{d}t$ is the number of moles of the gas released upon dissociation of the hydrate per unit time (hydrate dissociation rate)/s^{-1}; K is the rate constant for dissociation; $(q_\mathrm{eq} - q)$ is the driving force of hydrate dissociation, q_eq is the fugacity of the gas in equilibrium with the hydrate or the equilibrium concentration of the gas in water, q is the fugacity or concentration of the dissolved gas under the experimental conditions.

The hydrate dissociation in the case of multicomponent hydrate-forming gas has been investigated.[133] It has been shown[136] that dissociation of pressed methane hydrate samples under the action of an aqueous solution of methanol cannot be described considering only the intrinsic reaction kinetics, but is described adequately in terms of models in which heat transfer is the rate-limiting stage. Other studies are devoted to dissociation of pellet-shaped methane hydrate samples placed into solutions of ethylene glycol or in silicone oil[137] and to dissociation of the hydrate formed in the pores of active carbon.[138] A numerical theoretical approach to the description of the intrinsic kinetics of hydrate dissociation assuming a two-stage mechanism of these processes has been developed.[139, 140] The guest evaporation from cavities near the surface was considered as the first stage, and fusion of the empty cavities thus formed was taken as the second stage. Hydrate dissolution under natural conditions (in deep-water basins) has been considered.[141–146] The data presented in various publications are in reasonable agreement with one another. The dissolution of hydrates was shown to be controlled by diffusion. A study of the effect of ultrasonic treatment on the dissociation of tetrafluoroethane hydrate demonstrated[147] that sonication accelerates dissociation more efficiently than the supply of an equivalent quantity of energy as heat. A detailed review of the dissociation models for natural gas hydrates and their applications has been reported.[148]

III.4. Hydrate formation in emulsions of water in organic liquids

A publication[149] addresses the formation of CCl_3F hydrate from water in oil emulsions. The results indicate that a hydrate shell is first formed around the emulsion drops and then becomes thicker. The process includes three stages: diffusion of the hydrate-forming gas from the emulsion surface towards the water drop; relatively slow hydrate nucleation on the surface of an emulsion drop; growing and thickening of the hydrate shell on the drop. The rate-limiting stage of the process is the transfer of the hydrate-forming gas from the gas phase to the water drop surface (diffusion through a layer of the hydrophobic liquid and hydrate crust). Experimental data have been obtained on the kinetics of formation of methane hydrate in an emulsion of water in diesel fuel over a broad water concentration range.[150] A mathematical model has been proposed, satisfactorily describing the rate of methane hydrate formation in the emulsion with the assumption that the process is rate-limited by the intrinsic kinetics of hydrate formation on the drop surface and by heat transfer. The hydrate formation rate was found to increase with increasing water content in the emulsion, in all probability, owing to an increase in the water/diesel contact area. As could be expected, in terms of known models, the rate of hydrate formation increases with increasing driving force of the process — supercooling or pressure excess over the equilibrium pressure. Experimental data[151] obtained for a 30% emulsion of water in octane were described on the basis of a model that assumes the simultaneous nucleation of the hydrate on the surface of all water drops and formation of one hydrate nucleus in each drop. The intrinsic kinetics of hydrate formation and the hydrate-forming gas transfer from the organic phase to the growing hydrate were considered as rate-limiting factors. The rate of mass transfer was assumed to depend on the hydrate content in the system. Generally, kinetic issues of hydrate formation in the emulsions have not yet been elaborated sufficiently thoroughly.

III.5. Effect of compounds dissolved in water on the gas hydrate formation rate

The addition of small amounts of some surfactants to water markedly changes the morphology and mechanism of gas hydrate formation. This effect was discovered for the first time by Kutergin *et al.*[152] Instead of formation of an impermeable hydrate film at the gas/water interface, in the presence of surfactants, hydrate particles form a loose mass,

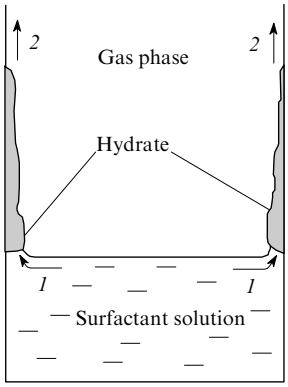


Figure 14. Chart of formation and growth of gas hydrates from a surfactant solution at the reactor side wall.[153]
(*1*) Capillary suction of a surfactant solution from the liquid phase bulk to reactor walls; (*2*) direction of the hydrate crystallization front.

which is saturated with the surfactant solution (like snow impregnated with melt water) and grows on the reactor walls (Fig. 14). This loose mass provides fast capillary suction of a surfactant solution into the reaction zone and increases the gas/liquid contact area (or the contact line of the liquid, hydrate and gas). The retention of the free water surface and the capillary suction of water into the reaction zone bring about a many-fold acceleration of hydrate formation and (in some cases) an almost 100% conversion of water to the hydrate. Recently, data have been reported on the formation of an intermediate solid phase with a low content of gas molecules in the presence of surfactants;[154] however, to confirm these results, additional investigations are required.

The ability of surfactant solutions to enhance the hydrate formation was utilized in many patented methods

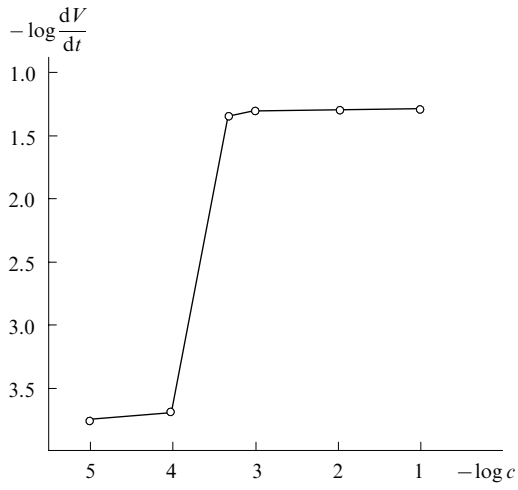


Figure 15. Effect of the concentration of sodium dodecyl sulfate [c (mass %)] on the growth rate of propane hydrates (litre min^{-1}).[22]
The driving force $RT\ln(P/P_{eq})$ = 1300 J mol^{-1}, T = 274 K; R is the universal gas constant; V is the volume of the absorbed gas (litres) at P = 0.1 MPa and T = 273.15 K; t is time/min.

for the preparation of large amounts of gas hydrates. Hydrate formation from surfactant solutions has been investigated.[155–162] It was shown that at low surfactant contents, the hydrate formation rate increases with increasing surfactant concentration and later this dependence reaches a plateau[22,155] (Fig. 15). The equilibrium conditions of hydrate formation do not depend on the presence of surfactants.[152,153,156] It was found[163] that micelle formation in surfactant solutions also does not influence the equilibrium conditions of hydrate formation and that not any surfactant changes the process rate. Indeed, the hydrate formation rate barely changes upon the addition of sodium oleate to the solution. According to a publication,[164] in the presence of non-ionic surfactants, methane and CO_2 hydrates grow as a dense film, whereas the addition of anionic surfactants induces the growth of a loose hydrate mass on the reactor walls. The mechanism of influence of surfactants on the hydrate formation is still not ultimately clear; however, it is obvious that the observed effect is due to the sorption of surfactant molecules on the surface of hydrate particles and a change of their surface properties.[156,158] There are also data that the induction time of hydrate formation may decrease in the presence of a surfactant in the aqueous phase.[158,160] Quite a few papers addressing the effect of surfactants on the hydrate formation have been surveyed in a review.[165] Note that not only surfactants, but also some salts present in solutions in low concentrations can accelerate the hydrate formation. It was demonstrated[166] that sodium halides dissolved in water in low concentrations accelerate the growth of methane hydrate; this effect is most pronounced with bromide and iodide. Similar results were obtained for the formation of CO_2 hydrate.[167] Some other substances, *e.g.*, amino acids and lower alcohols may act similarly to surfactants.[168–170]

One more type of additives that are currently actively studied are so-called kinetic hydrate inhibitors (KHIs), which are used in oil production. These additives are the subjects of several reviews.[171–174] The addition of ~1 mass % KHIs to the aqueous phase sharply increases the induction time of hydrate formation. Therefore, the multiphase flow (water–oil–gas) moving along a pipeline has time to pass the part susceptible to hydrate formation without forming the hydrate. Initially, the study of KHIs was initiated by the discovery of proteins that inhibit ice formation in the blood of some insects and fishes, which allows the living organisms to survive at temperatures below the freezing point of water. Most of modern KHIs belong to two groups of water-soluble polymers — vinylcaprolactam polymers (or copolymers) and hyperbranched poly(ester-amide)s. They operate satisfactorily at moderate driving forces of the hydrate formation (< 10 K).

No unambiguous views on the mechanism of action of KHIs have been formed to date. The following key mechanisms have been proposed:

— destabilization of the hydrate phase nuclei by KHIs (this mechanism implies that particularly nucleation of the hydrate phase is hampered);

— adsorption of KHIs on the surface of hydrate particles, resulting in retardation or termination of their growth (the nuclei are formed but cannot grow);

— adsorption of KHIs on the surface of particles that serve as heterogeneous nucleation sites in the aqueous phase, leading to suppression of heterogeneous nucleation.

A number of reasons supporting the first mechanism have been reported, for example, by Del Villano *et al.*[175] The sorption of KHIs on the hydrate particles was many times demonstrated to occur. This is indicated by the change in the morphology of the hydrate particles that grow from solutions of KHIs in comparison with the morphology of hydrates that grow without KHIs.[176,177] The isotherms of sorption from aqueous solutions of polyvinylpyrrolidone (PVP) and polyvinylcaprolactam (PVC) on hydrate particles have been measured.[178] It was found that PVP tends to form sorbed monolayers, while PVC is prone to multilayer sorption. This was regarded to be responsible for the higher PVC activity as a kinetic inhibitor. Facts supporting the third mechanism have also been reported;[179] correlations have been found between the ability of PVP and PVC to be sorbed on the SiO_2 surface, characteristics of the resulting layer and the KHI activity. Probably, the mechanisms of action of various KHIs can be different.

Not only synthetic polymers, but also natural proteins can function as KHIs.[179–182] The inhibition of ice formation is associated with the sorption of these proteins on the ice surface; ice growth between protein globules becomes difficult. A sorbed protein film was found on the surface of hydrate particles and the effect of proteins on the hydrate crystal morphology and the hydrate formation rate was considered.[180] This type of KHIs affects little the homogeneous nucleation, but is does affect the heterogeneous nucleation (protein molecules are sorbed on the surface of suspended particles that serve as the nuclei for the hydrate formation) and the growth of hydrate particles (protein molecules are sorbed on their surface). The sorption of various KHIs on the SiO_2 surface has been investigated.[181] The authors formulated the requirements for a KHI layer to have a high inhibitory efficiency: the layer should be rigid, strongly bound to the surface and possess a large adsorption mass (be sufficiently thick). It was proposed to use the results of sorption investigations for fast evaluation and selection of potential KHIs. The conclusions made by the researchers[181] coincided with the opinion expressed in a work[183] devoted to the application of various types of modified starches as KHIs. Among tested compounds, considerable activity was exhibited only by the starch tapioca (extracted from the cassava root); its inhibitory activity increased in the presence of poly(ethylene oxide). The authors arrived at the conclusion that the effect of KHIs is associated with sorption on the heterogeneous nucleation sites.

Recent studies of hydrate formation in a stirred reactor in the presence of KHIs have demonstrated[184] that inhibitors not only extend the induction time, but also retard the growth of hydrates. The effect of KHIs (mainly natural proteins) on the growth rate of the hydrate was studied by Jensen *et al.*[185] It was found that in the presence of KHIs, the hydrate formation rate decreases. In the case of relatively high concentrations of KHIs, two stages can be clearly distinguished in the kinetic curve — the first slower (initial) stage and the second faster stage. The authors attributed this to the sorption of KHIs on the surface of growing hydrate particles, which is responsible for retarded hydrate formation. The switching from the first stage to the second one is associated with the decrease in the KHI concentration in the solution.

Furthermore, dissociation of hydrates is accelerated in some cases in the presence of KHIs. The use of NMR to study the formation of hydrates in the presence of KHIs and the mechanism of action of KHIs have been considered.[186] It was shown[187] that a classical KHI — polyvinylpyrrolidone — barely affects the hydrate formation rate when present in 10 ppm concentration in an aqueous solution and decreases the rate by approximately an order of magnitude when present in 1000 ppm concentration. This behaviour was attributed[188] to decreasing surface area of hydrate particles accessible for the addition of hydrate building units.

In a calorimetric study,[189] it was shown that the presence of KHIs in aqueous solutions may increase or decrease the equilibrium temperature of hydrate dissociation by several degrees. The authors attributed this to the formation of hydrates of different compositions. The same researchers demonstrated[190] that the hydrate formation from a mixture of hydrocarbons in the presence of KHIs is accompanied by a change in the filling of hydrate cavities by guest molecules. In particular, the content of heavy components in large cavities can increase, which would increase the temperature of hydrate dissociation.

III.6. Formation and dissociation of hydrates at temperatures < 273 K

The formation processes of gas hydrates at temperatures below the water freezing point have been studied in a number of papers.[191–193] The reaction occurred between ice particles of nearly spherical shape and the gas. This interaction was described in most detail by Kuhs and coworkers.[193,194] The resulting experimental curves were analyzed resorting to kinetics of heterogeneous reactions. Hydrate nuclei were found to appear in the first stage of the process on some surface sites of ice particles. These nuclei grow and gradually cover the whole surface. After the surface of ice particles has been completely covered with the hydrate, the boundary between ice and the formed hydrate shell starts to be displaced towards the interior of the ice particle in accordance with the known 'contracting sphere' model. Note that for accelerating the hydrate formation and achieving the thermodynamic equilibrium, it is necessary to mechanically destroy the hydrate crust, for example, by metallic beads placed in the reactor.[195,196]

It was found[197] that the hydrate nucleus formed upon the interaction of ice and xenon gas is characterized by a higher content of small cavities than the bulk hydrate phase, *i.e.*, they are structurally non-equivalent. Therefore, the hydrate formation rate can be controlled by both gas diffusion towards the reaction surface through the hydrate layer and the proper hydrate formation rate. Attention is attracted by high activation energy for methane diffusion through a hydrate layer — 52.1 kJ mol^{-1} (Ref. 193), which attests to low porosity of the hydrate crust. For the formation of the CO_2 hydrate, the activation energies were determined to be 46 and 19 kJ mol^{-1} for temperatures above and below 225 K, respectively.[194] The authors attributed this difference to a change in the mechanism of transport of the hydrate-forming gas on temperature change. The mathematical model of hydrate formation from ice is considered in the same publication. The results of NMR studies of hydrate formation from ice and a methane – propane mixture[198] are consistent with the above mechanism (diffusion of hydrate-forming gas molecules through

the hydrate layer as the rate-limiting step). The signal of propane in large cavities was found to increase more rapidly than the signal of methane in small cavities (taking account of the known hydrate composition). Apparently, this implies the formation of hydrate, in which not all of the small cavities are occupied by methane.

The situation where the rate of the dissociation reaction A(solid) → B(solid) + gas is limited by the removal of the gas formed through the solid layer of the product to the surface of the initial compound is well-known in the kinetics of heterogeneous reactions. The dissociation of gas hydrates at temperatures < 273 K follows the same mechanism. According to results of numerous studies,[199–206] upon dissociation, hydrate particles are covered by an ice crust, which considerably retards the reaction. The gas diffusion through the ice crust is the rate-limiting stage. For sufficiently large monolithic particles of some hydrates, the retardation of dissociation by the ice crust is so pronounced that it has acquired a special name — self-preservation [199–201] (or anomalous preservation) [202] of gas hydrates. The hydrate preservation by means of ice was first mentioned in a paper [207] devoted to calorimetric measurements of thermophysical properties of gas hydrates. It was noted that at temperatures < 273 K, the dissociation of xenon and krypton hydrates is not complete. The authors suggested that dissociation of a part of the hydrate gives rise to an insulating ice coat on its surface, which prevents further dissociation. The first detailed studies of the self-preservation of gas hydrates (in relation to methane hydrate and the ice–hydrate agglomerate) were performed by a Russian research team in 1986–1987.[199, 200, 208] It was found that depending on the texture (monolithic hydrate, ice–hydrate agglomerate, porous hydrate), samples had different stability under the same storage conditions outside the thermodynamic stability region of hydrates. The needle and whisker crystals of the hydrate dissociated very rapidly — within 2–3 min to 5–6 days, depending on the size. The massive porous hydrate completely dissociated within two weeks. The gas content of the monolithic hydrate decreased by $\sim 30\%$ on storage for > 5 months ($T = 263–268$ K). The gas content of ice–hydrate samples, obtained by freezing methane-saturated water under hydrate formation conditions and containing several percent of the hydrate, virtually did not change on storage at 267 K for one and a half years.

Below we consider experimental data on the self-preservation of the hydrates. Experiments performed by a Japanese research team [204, 206] have demonstrated that at temperatures > 189 K, dissociation of methane hydrate consists of two stages: first (in the initial 10 min), the hydrate dissociates rather actively, and then the dissociation rate sharply decreases as a result of a hexagonal ice crust formation on the hydrate surface. Further dissociation of the hydrate is dictated by the conditions of methane diffusion through the pores or ice crystallite boundaries. According to numerical estimates, the effective coefficients of methane diffusion through the ice crust were 2.2×10^{-11} and 8.7×10^{-11} m^2 s^{-1} for temperatures of 189 and 198 K, respectively.

Takeya *et al.*[203] studied the dependence of the methane hydrate dissociation rate on the hydrate particle size. Polycrystalline methane hydrate samples were heated from 135 to 263 K at a rate of 1 K min^{-1} under atmospheric pressure. The hydrate particles of up to 250 μm size completely dissociated below 210 K. The 1000–1400 μm particles contained $\sim 20\%$ of hydrate even at 263 K. A microstructural study using a confocal scanning microscope detected ice on the hydrate surface after partial dissociation. It has been shown [205] that at a temperature of 193 K (the equilibrium temperature of methane hydrate dissociation at 0.1 MPa), the hydrate surface starts to be covered with a multitude of fine ice particles and on further heating to ~ 210 K, no visible changes are observed. On subsequent temperature rise to 230 K, fine ice particles are sintered and the surface is coated by continuous ice crust, which prevents hydrate decomposition.

It has been shown [209] that not only the temperature, but also the pressure of ice crust formation is significant for self-preservation. The efficiency of self-preservation was found to be affected by the initial ice microstructure and the degree of consolidation of ice hydrate particles. The optimal self-preservation parameters found in this work are $T = 250$ K and $P = 0.7$ MPa. The presence of ice impurity in the initial hydrate particles has been found [210] to enhance their self-preservation. A comprehensive examination of the nature of self-preservation was reported, for example, by Istomin *et al.*[201] A mechanism of hydrate self-preservation with metastable liquid water being the intermediate phase has been proposed.[199, 200, 208] Experimental evidence for the intermediate formation of liquid water during the dissociation of hydrates at temperatures < 273 K was obtained quite recently.[211]

An US research team [202] disclosed a considerable dependence of the efficiency of self-preservation of methane hydrate on temperature and on the way of transfer to the non-equilibrium state. Temperature ramping at a rate of 10 K h^{-1} and a sharp pressure decrease below the equilibrium value were considered. The self-preservation (called anomalous preservation by the authors) was observed only upon a pressure decrease. As pressure was decreased to 0.1 MPa in the temperature range of 195–240 K, the rate of dissociation of the hydrate increased monotonically with

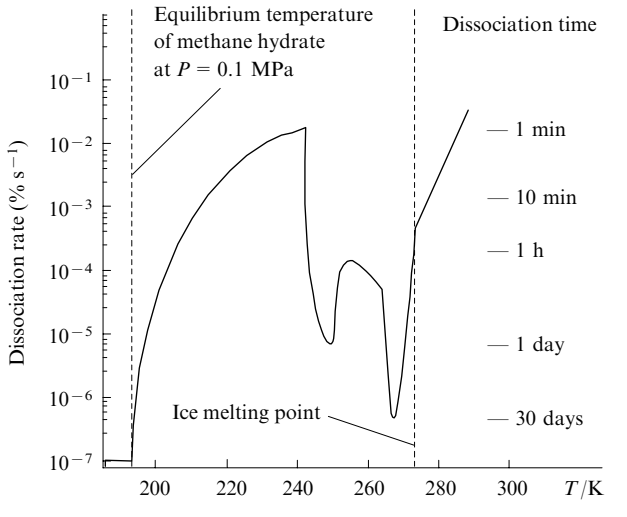


Figure 16. Average rate and time of half dissociation of methane hydrate sample at $P = 0.1$ MPa and different external temperatures.[202]

temperature rise, while in the temperature range of 240–271 K, the temperature dependence of the dissociation rate passed through a deep minimum (Fig. 16). It is noteworthy that the value of 240 K is close to the homogeneous nucleation temperature of water (the minimum temperature to which liquid water can be supercooled).

Considering the formation of liquid water as an intermediate phase during decomposition of the hydrate into ice and gas,[211,212] it can be assumed that the anomalous dissociation pattern in the temperature range of 240–272 K is related to the change in the mechanism of formation of hexagonal ice on the surface of hydrate particles upon dissociation. Melnikov *et al.*[20] demonstrated that for methane hydrates, the formation of supercooled water at $P = 0.1$ MPa and $T < 240$ K is thermodynamically impossible. Under these conditions, the dissociation of methane hydrate into ice and gas should follow the mechanism of direct solid-phase transition in which the formation of a continuous ice crust can hardly be suggested. Rather, single crystallites would appear on the surface of hydrate particles without forming a continuous coating. At temperatures > 240 K and pressure of 0.1 MPa, methane hydrate can dissociate into the gas and metastable liquid water. In this case, water that wets the hydrate surface would form a continuous film on the hydrate particles. This film is frozen to give an impermeable protective ice crust, which prevents release of the gas from the hydrate. This mechanism of appearance of an impermeable ice crust on the hydrate surface proposed by Melnikov *et al.*[20] is consistent with the experimental data considered in the previous paragraph.

Some recent publications demonstrate that hydrates can dissociate without the formation of an ice shell. According to X-ray computed tomography studies,[213] decomposition of krypton hydrate affords a mixture of the hydrate and ice, whereas dissociation of argon hydrate affords the ice crust on the surface of hydrate particles. As the ice crust grows, the rate of dissociation of the argon hydrate gradually decreases, whereas in the case of krypton hydrate, the formation of an ice–hydrate mixture leads to fast self-preservation of the remaining minor part of the hydrate.

IV. Methods for studying the formation and dissociation kinetics of gas hydrates

The formation and dissociation of gas hydrates are studied using a broad range of modern physicochemical methods; however, the key method is still the measurement of the amount of the gas absorbed upon hydrate formation or released upon hydrate dissociation at controlled pressure and temperature values, so-called $P-V-T$ measurements. If the temperature and pressure of the system do not chnge too much during the process, the composition of the resulting hydrate can be considered invariable. Hence, the quantity of formed (dissociated) hydrate is directly proportional to the quantity of the absorbed (released) gas and can be easily calculated. Measurement of the pressure decrease upon hydrate formation and the pressure increase upon hydrate dissociation is a version of this method. Using the equation of state, it is possible to calculate the quantity of absorbed (evolved) gas. More kinetic information can be gained by other methods, which are briefly considered below.

IV.1. Optical microscopy

Optical microscopy is a direct method for monitoring processes on a real time scale. In a large number of studies, optical microscopy was used to monitor the formation and growth of hydrate crystals.[20,94–101,103–105,203,214] This method can serve to examine the morphology and macroscopic details of the growth of hydrate particles and the rates of building-up of the hydrate film at the gas/water interface. As a rule, experiments of this type are carried out using a high-pressure reactor with two optical windows located opposite to each other, which allows observations in a 'transmission' geometry. The operation of modern automated instrumentation for studying the nucleation of hydrates at the gas/water interface is based on the optical recording of the hydrate formation moment, *i.e.*, actually this is a sort of optical microscopy application (see, for example, Ref. 58). Examples of using electron microscopy to study hydrates are also available.[192,193]

IV.2. Thermal and calorimetric methods

A relatively simple method based on the measurement of sample temperature is widely used for the qualitative and semiquantitative detection of the onset or progress of hydrate formation and dissociation (for various versions of thermal analysis, see, for example, Ref. 215). This approach is based on the fact that hydrate formation is an exothermic process, while hydrate dissociation is endothermic. A measuring probe located near or inside the sample detects a temperature step at the onset of hydrate formation. A good example of application of this method is the detection of hydrates in geological samples brought to the surface. Even if the hydrate has completely decomposed during delivery to the surface, the presence of cold spots in the sample attests to the presence of hydrates.[216]

Quantitative information about the hydrate formation is gained using the calorimetric method by measuring the heat evolved upon hydrate formation or absorbed upon hydrate dissociation as a function of time or sample temperature. Since the evolved heat is proportional to the amount of hydrate formed and the enthalpy of formation of most hydrates is known, the calorimetric method can serve for determining the total amount of hydrate that has formed (or dissociated) in the system and the pattern of hydrate accumulation (consumption). For example, the kinetics of methane hydrate nucleation and growth in simulated drilling fluids has been studied by calorimetry.[217,218]

IV.3. Diffraction methods

Powder X-ray and neutron diffraction can be used in kinetic measurements. In the case of a perfectly prepared sample, the intensity of reflections of the crystalline phase in the powder X-ray diffraction patterns is proportional to the amount of this phase in the sample. This correlation underlies quantitative diffraction methods. It is noteworthy that diffraction methods provide information not only on the number of phases in the sample, but also on the phase composition. This type of information is, as a rule, of interest by itself. The above-mentioned requirement of 'perfect' sample preparation imposes considerable limitations on the applicability of diffraction methods for kinetic measurements. Indeed, one of the major requirements for the use of diffraction methods is the presence of crystallites with all possible spatial orientations; furthermore, all orientations must be equally probable. Because of rather low

penetration ability of X-rays, the volume of the sample involved in the diffraction is usually moderate (of the order of several cubic millimetres). This condition can hardly be fulfilled in the powder diffraction studies of hydrate kinetics. The volumes of samples used in the neutron diffraction method are several cubic centimetres; therefore, it is this method that was used to study the formation kinetics of hydrates from ice and a gas.[191 – 193]

IV.4. Nuclear magnetic resonance spectroscopy

Nuclear magnetic resonance spectroscopy (NMR) is a powerful tool for investigation of gas hydrates. The position of a signal in the NMR spectrum is very sensitive to the environment of the molecule containing the test nucleus, which makes it possible to distinguish between guest molecules located in different types of cavities. The signal intensity in the NMR spectrum is proportional to the total number of nuclei of a particular sort. This method provides information on the whole sample volume. However, the examples of using NMR spectroscopy for kinetic investigations of hydrate formation and dissociation are still few. This may be due to high cost of the equipment and to complexity of adjusting the equipment to measurements at elevated pressures. Nevertheless, NMR spectroscopy has been successfully used to study the formation of xenon hydrate from ice[197] and a mixed methane and propane hydrate.[198] The main value of the results obtained in these works is related to nucleation and growth mechanisms rather than to the hydrate formation rate. ^{1}H NMR relaxation measurements have been used to follow the dynamics of Freon hydrate formation and dissociation.[219]

IV.5. Raman spectroscopy

Raman spectroscopy is widely used to study gas hydrates.[220, 221] The characteristic vibrational frequencies of the guest molecules are known to change somewhat depending on their environment; therefore, it is possible to reliably measure the frequencies for molecules located in small and large cavities of hydrates and molecules dissolved in the water bulk. From the intensity ratio of Raman spectral bands, it is possible to determine the occupancy ratio of large and small hydrate cavities and the percentage of molecules not incorporated in the hydrate. However, this method provides information about a rather small volume, which cannot adequately represent the whole sample. There are examples of successful use of Raman spectroscopy for studying the mechanism of formation of methane hydrate.[33]

IV.6. Nephelometry

The hydrate formation and growth processes can be studied by methods based on light scattering. The simplest method applicable for this purpose is nephelometry, which is based on measurement of the intensity of light scattered at a particular angle.[222, 223] For example, this method has been used[222] for studying the induction times of hydrate formation in the water – ethane system. The onset of hydrate formation in the solution was detected by an increase in the light scattering intensity. Nephelometry has also been used to study the effects of various added particles on the hydrate formation. For example, particles with positively and negatively charged surfaces were added to a solution saturated with gases. After the onset of hydrate formation, the scattered light intensity increased with time; this made it possible to study the time dependences of this process. Using this approach, it was, in particular, found that positively charged particles virtually did not affect the induction time, whereas negatively charged particles decreased the induction time almost twofold.[222]

Nephelometry can also be used to detect the onset of hydrate formation, to study the growth rate of the hydrate mass and to determine the hydrate composition. However, it does not provide information about characteristics of crystals formed in solutions such as the size and concentration. Meanwhile, this information is very important for the understanding of hydrate formation processes and, hence, it should be gained by other methods.

IV.7. Static light scattering

Static light scattering (often called laser diffraction) can be applied for determination of the sizes and concentrations of hydrate particles formed in solution.[224, 225] The method is based on analysis of the angular dependence of the intensity of laser radiation scattered by the sample. This method can be applied on a real time basis to study the kinetics of nucleation of the new phase. However, it proved to be efficient for tens (or more) of micrometre-sized particles, whereas for particles of less than one micrometre in size, the method is inapplicable. For calculation of the hydrate particle size, it is also necessary to know the refractive index of the hydrate crystal, which should be determined by other experimental and theoretical approaches.[22, 226, 227, 228]

IV.8. Multi-wavelength extinction

Multi-wavelength extinction technique, which consists in measuring the turbidity from the decrease in the intensity of light after it has been passed through the sample (turbidimetry) is also applicable for measuring the size and concentration of hydrate particles.[22, 118, 226] The turbidity is measured at several wavelengths, which accounts for the name of the method. For example, a procedure has been developed[22] for determining the size and concentration of hydrate particles in the solution by measurement of the turbidity at two wavelengths. This procedure was suitable for determining the average size and concentration of particles of various gas hydrates on a real time basis, but the hydrate particles could be detected only starting from the size of several micrometres. Furthermore, as in the case of laser radiation diffraction, refractive indices of the hydrate crystals should be known for the use of this method.

IV.9. Focused beam reflectance

The focused beam reflectance method has been used[107 – 110] to determine the sizes and concentrations of hydrate particles. Using this method, particle size distribution was assessed and the concentration of hydrate particles in the aqueous phase was determined. However, like for other optical methods, the range of sizes accessible for measurements is confined by the diffraction limit. As a result, the minimum detectable size is ~ 1 μm.

IV.10. Dynamic light scattering

Currently, dynamic light scattering is efficiently used to determine the nanoparticle size in colloidal systems. Using this method, it is possible to determine the average hydrodynamic diameter of particles and the particle size distribution (down to fractions of a nanometre). The particle size can be assessed without knowing the refractive index, which

is required in the case of laser diffraction and turbidimetry. For correct determination of the hydrodynamic particle size, it is necessary to know the viscosity and the refractive index of the medium. For water and most aqueous solutions, these values are well-known over a broad temperature range or, if necessary, they can be easily found experimentally.

Yousif *et al.*[229] described an instrument for investigation of the formation and growth of gas hydrates on the basis of dynamic light scattering. However, the results of application of this method to real systems have not been reported.

Uchida *et al.*[230] used dynamic light scattering to measure the dynamic viscosity of water saturated with CO_2, *i.e.*, they solved the inverse problem; particles of a known size were added to water and the unknown viscosity was thus determined. It was found that after a definite point of time, after solution cooling and saturation with the gas, the viscosity started to increase to reach a value $\sim 15\%$ higher than the characteristic value for water at the given gas saturation. Since the temperature and pressure at which the viscosity measurement was carried out corresponded to the gas hydrate formation conditions, the authors attributed the increase in the viscosity to preparation of water for hydrate formation, with some 'hydrate-like' structures being formed. Meanwhile, no real gas hydrate particles were detected.

To the best of our knowledge, there are no reported cases of successful use of dynamic light scattering to study the formation and growth of hydrate particles from a gas-saturated aqueous solution. Probably, this is mainly caused by the specific nature of this method in which the particle size is derived from the measured displacement of particles caused by Brownian motion. It is important to eliminate any flows, which would give rise to additional Brownian motion of particles in the sample. Hence, this method is inapplicable to hydrate formation processes in stirred vessels. For measurements without stirring, it is still necessary to envisage special measures to eliminate convective flows arising upon cooling of the samples.

V. Conclusion

The kinetic characteristics of the formation and dissociation of gas hydrates are critical for understanding of the behaviour of both man-made and natural gas hydrates. This review covers data of the last 10–15 years on the nucleation, growth and dissociation of hydrates. The results of studies of the morphology of the formed hydrate crystals were analyzed, as well as the factors that affect the hydrate formation, that is, change the induction time and growth rate of crystals. In the vast majority of studies, hydrate formation processes were detected at later stages when single particles had macroscopic size.

For further development of research along this line, it seems relevant to study the nucleation and growth of gas hydrates in early stages with real-time recording of the size, morphology and the number of hydrate particles. It is crucially important to learn to detect and control crystallization processes in the nanometre range. For investigation of hydrate nanoparticles and selection of parameters, the variation of which would provide control over the particle number and size in the initial stages of growth, it is necessary to find appropriate methods for detecting and monitoring the hydrate growth processes.

Among the modern experimental approaches, none are suitable for monitoring the hydrate formation processes at early stages and for gaining information about the size and concentration of the hydrate particles formed. Dynamic light scattering, which is able to determine the particle size in the range from 1 nm to several micrometres in the liquid seems to be the most promising method for investigating the early stages of hydrate formation; it is also possible to use additionally other optical methods such as optical microscopy, turbidimetry, static light scattering and so on.

The review was written with the financial support of the Advanced Research Foundation.

References

1. V A Istomin, V S Yakushev *Gazovye Gidraty v Prirodnykh Usloviyakh* (Gas Hydrates under Natural Conditions) (Moscow: Nedra, 1992)
2. E D Sloan, C A Koh *Clathrate Hydrates of Natural Gases* (3rd Edn) (Boca Raton, London, New York: CRC Press, 2008)
3. V A Istomin, V G Kvon *Preduprezhdenie i Likvidatsiya Gazovykh Gidratov v Sistemakh Dobychi Gaza* (Prevention and Elimination of Gas Hydrates in Gas Production Systems) (Moscow: IRTs Gazprom, 2004)
4. J Carroll *Natural Gas Hydrates: A Guide for Engineers* (Gulf Professional Pub., 2003)
5. V G Vasil'ev, Yu F Makogon, F A Trebin, A A Trofimuk, V G Cherskii *Otkrytiya, Izobreteniya, Promyshlennye Obraztsy, Tovarnye Znaki* **10** 4 (1970)
6. A Yu Manakov, A D Duchkov *Russ. Geol. Geophys.* **58** 240 (2017)
7. Yu F Makogon *Ros. Khim Zh.* **47** (3) 70 (2003)
8. Y F Makogon, S A Holditch, T Y Makogon *J. Petrol. Sci. Eng.* **56**14 (2007)
9. V A Solov'ev *Ros. Khim. Zh.* **47** (3) 59 (2003)
10. Z R Chong, S H B Yang, P Babu, P Linga, X S Li *Appl. Energy* **162** 1633 (2016)
11. V S Yakushev P*rirodnyi Gaz i Gazovye Gidraty v Kriolitozone* (Natural Gas and Gas Hydrates in the Permafrost Zone) (Moscow: GAZPROM-VNIIGAZ, 2009)
12. A M Mastepanov *Ekologicheskii Vestnik Rossii* (4) 20 (2015)
13. V S Yakushev, V G Kvon, Yu A Gerasimov, V A Istomin *Sovremennoe Sostoyanie Gazogidratnykh Tekhnologii. Obzornaya Informatsiya* (Current State of Gas Hydrate Technology. Overview Information) (Moscow: IRTs Gazprom, 2008)
14. V S Yakushev, V G Kvon, S I Dolgaev, V A Istomin *Analiz Konkurentnykh Preimushchestv Gidratnykh Tekhnologii v Gazovoi Promyshlennosti. Analitik-2009: Sbornik Nauchno-Tekhnicheskikh Obzorov* (Analysis of the Competitive Advantages of Hydrate Technology in the Gas Industry. Analyst-2009. Collection of Scientific and Technical Reviews) (Moscow: Gazprom-VNIIGAZ, 2010)
15. J Javanmardi, M Moshfeghian *Appl. Therm. Eng.* **23** 845 (2003)
16. V M Vorotyntsev, V M Malyshev *Russ. Chem. Rev.* **80** 971 (2011)
17. K A Birkedal, L P Hauge, A Graue, G Ersland *Energies* **8** 4073 (2015)
18. T Arunyanart, U Siripatrawan, S Takeya, H Noritake, Y Makino, S Oshita *J. Food Eng.* **165** 104 (2015)
19. A Yu Manakov, Doctoral Thesis in Chemical Sciences, Institute of Inorganic Chemistry, Siberian Branch of the RAS, Novosibirsk, 2007
20. V P Melnikov, A N Nesterov, A M Reshetnikov, V A Istomin, W G Kwon *Chem. Eng. Sci.* **65** 906 (2010)

21. P R Bishnoi, V Natarajan *Fluid Phase Equilib.* **117** 168 (1996)
22. A N Nesterov, Doctoral Thesis in Chemical Sciences, Iinstitute of Earth Cryosphere, Siberian Branch of the RAS, Tyumen, 2006
23. C P Ribeiro Jr, P L C Lage *Chem. Eng. Sci.,* **63** 2007 (2008)
24. L Boewer, J Nase, M Paulus, F Lehmkuhler, S Tiemeyer, S Holz, D Pontoni, M Tolan *J. Phys. Chem. C* **116** 8548 (2012)
25. P Warrier, M N Khan, V Srivastava, C M Maupin, C A Koh *J. Chem. Phys.* **145** 211705 (2016)
26. J A Ripmeester, S Alavi *Curr. Opin. Solid State Mater. Sci.* **20** 344 (2016)
27. A Nilsson, L G M Pettersson *Chem. Phys.* **389** 1 (2011)
28. I Brovchenko, A Geiger, A Oleinikova *J. Chem. Phys.* **123** 044515 (2005)
29. P Buchanan, A K Soper, R E Westacott, J L Creek, C A Koh *J. Chem. Eng. Data* **48** 778 (2003)
30. C A Koh, R P Wisbey, X Wu, R E Westacott, A K Soper *J. Chem. Phys.* **113** 6390 (2000)
31. A Filipponi, D T Bowron, C Lobban, J L Finney *Phys. Rev. Lett.* **79** 1293 (1997)
32. B Muller-Bongartz, T R Wildeman, E D Sloan, in *The Proceedings of the Second International Offshore and Polar Engineering Conference, San Francisco, 1992* p. 628
33. S Subramanian, E D Sloan *Fluid Phase Equilib.* **158 – 160** 813 (1999)
34. J M Schicks, M Luzi-Helbing *J. Chem. Eng. Data* **60** 269 (2015)
35. Y Bi, T Li *J. Phys. Chem. B* **118** 13324 (2014)
36. Y Bi, A Porras, T Li *J. Chem. Phys.* **145** 211909 (2016)
37. G J Guo, Y G Zhang, H Liu *J. Phys. Chem. C* **111** 2595 (2007)
38. R W Hawtin, D Quigley, P M Rodger *Phys. Chem. Chem. Phys.* **10** 4853 (2008)
39. M R Walsh, C A Koh, E D Sloan, A K Sum, D T Wu *Science*. **326** 1095 (2009)
40. J A Ripmeester, S Alavi *ChemPhysChem.,* **11** 978 (2010)
41. S Liang, P G Kusalik *J. Phys. Chem. B* **117** 1403 (2013)
42. S A Bagherzadeh, P Englezos, S Alavi, J A Ripmeester *J. Phys. Chem. C* **116** 24907 (2012)
43. L C Jacobson, W Hujo, V Molinero *J. Phys. Chem. B* **114** 13796 (2010)
44. L C Jacobson, V Molinero *J. Am. Chem. Soc.* **133** 6458 (2011)
45. M Lauricella, S Meloni, N J English, B Peters, G Ciccotti *J. Phys. Chem. C* **118** 22847 (2014)
46. J Vatamanu, P G Kusalik *Phys. Chem. Chem. Phys.* **12** 15065 (2010)
47. D Kashchiev, A Firoozabadi *J. Cryst. Growth* **243** 476 (2002)
48. D Kashchiev, A Firoozabadi *J. Cryst. Growth* **250** 499 (2003)
49. D Kashchiev, A Firoozabadi *J. Cryst. Growth* **241** 220 (2002)
50. M R Anklam, A Firoozabadi *J. Chem. Phys.* **121** 11867 (2004)
51. V P Skripov *Metastable Liquids* (New York: Wiley, 1974)
52. D Knezic, J Zaccaro, A S Myerson *J. Phys. Chem. B* **108** 10672 (2004)
53. A F Heneghan, H J Moore, T R Lee, A D J Haymet *Shem. Phys. Lett.* **385** 441 (2004)
54. I Weidinger, J Klein, P Stockel, H Baumgartel, T Leisner *J. Phys. Chem. B* **107** 3636 (2003)
55. A F Heneghan, P W Wilson, A D J Haymet *Proc. Natl. Acad. Sci. USA* **99** 9631 (2002)
56. R Ohmura, M Ogawa, K Yasuoka, Y H Mori *J. Phys. Chem. B* **107** 5289 (2003)
57. K Lee, S-H Lee, W Lee *Int. J. Greenhouse Gas Control* **14** 15 (2013)
58. N Maeda, D Wells, P G Hartley, K A Kozielski *Energy Fuels* **26** 1820 (2012)
59. P W Wilson, D Lester, A D J Haymet *Chem. Eng. Sci.* **60** 2937 (2005)
60. V I Kosyakov, V A Shestakov *Izv. Sib. Otd. Akad. Nauk, Ser. Khim. Nauk* **5** 8 (1976)
61. R P Sear *CrystEngComm* **16** 6506 (2014)
62. A S Stoporev, A Yu Manakov, V I Kosyakov, V A Shestakov, L K Altunina, L A Strelets *Energy Fuels* **30** 3735 (2016)
63. N Maeda *Fluid Phase Equilib.* **413** 142 (2016)
64. N Maeda *Chem. Eng. Sci.* **155** 1 (2016)
65. N Daraboina, S Pachitsas, N von Solms *Fuel* **148** 186 (2015)
66. H Sharifi, J Ripmeester, V K Walker, P Englezos *Fuel* **117** 109 (2014)
67. S R Davies, K C Hester, J W Lachance, C A Koh, E D Sloan *Chem. Eng. Sci.* **64** 370 (2009)
68. M Sarshar, F Esmaeilzadeh, J Fathikaljahi *Oil Gas Sci. Technol.-Rev. D: IFP Energ. Nouvelles* **63** 657 (2008)
69. L Jensen, K Thomsen, N von Solms *Chem. Eng. Sci.* **63** 3069 (2008)
70. R Wu, K A Kozielski, P G Hartley, E F May, J Oxall *AIChE J.* **59** 2640 (2013)
71. W Shin, S Park, H Ro, D-Y Koh, J Seol, H Lee *Chem. Asian J.* **7** 2235 (2012)
72. H Ohno, I Moudrakovski, R Gordienko, J Ripmeester, W K Walker *J. Phys. Chem. A* **116** 1337 (2012)
73. S Sun, X Peng, Y Zhang, J Zhao, Y Kong *J. Chem. Thermodyn.* **107** 141 (2017)
74. S Dai, J-Y Lee, J C Santamarina *Fluid Phase Equilib.* **378** 107 (2014)
75. H Li, L Wang *Fuel* **140** 440 (2015)
76. J Wang, R Wang, R-H Yoon, Y Seol *J. Chem. Eng. Data* **60** 383 (2015)
77. S-D Zhou, Y-S Yu, M-M Zhao, S-L Wang, G-Z Zhang *Energy Fuels* **28** (7) 4694 (2014)
78. E Rezaei, M Manteghian, M Tamaddondar *J. Petrol. Sci. Eng.* **147** 857 (2016)
79. A N Nesterov, A M Reshetnikov, A Y Manakov, T V Rodionova, E A Paukshtis, I P Asanov, S P Bardakhanov, A I Bulavchenko *J. Mol. Liq.* **204** 118 (2015)
80. A Mohammadi, M Manteghian, A Haghtalab, A H Mohammadi, M R Abkenar *Chem. Eng. J.* **237** 387 (2014)
81. H Najibi, M M Shayegan, H Heidary *J. Nat. Gas Sci. Eng.* **23** 315 (2015)
82. H Pahlavanzadeh, S Rezaei, M Khanlarkhani, M Manteghian, A H Mohammadi *J. Nat. Gas Sci. Eng.* **34** 803 (2016)
83. H Kakati, A Mandal, S Laik *J. Ind. Eng. Chem.* **35** 357 (2016)
84. Q Wu, B Zhang *J. Nat. Gas Chem.* **19** 446 (2010)
85. P W Wilson, A D J Haymet *Chem. Eng. J.* **161** 146 (2010)
86. O Fandiso, L Ruffine *Fuel* **117** 442 (2014)
87. T Uchida, K Yamazaki, K Gohata *J. Phys. Chem. C* **120** 26620 (2016)
88. B Sowa, N Maeda *J. Phys. Chem. A* **119** 10784 (2015)
89. E P Zaporozhets, N A Shostak *Neftepromyslovoe Delo* (1) 49 (2015)
90. J Zhao, K Xu, Y Song, W Liu, W Lam, Y Liu, K Xue, Y Zhu, X Yu, Q Li *Energies* **5** 399 (2012)
91. V P Voronov, E E Gorodetskii, A R Muratov *J. Phys. Chem. B* **114** 12314 (2010)
92. A Falenty, J Qin, A N Salamatin, L Yang, W F Kuhs *J. Phys. Chem. C* **120** 27159 (2016)
93. C M R Yonkofski, J A Horner, M D White *J. Nat. Gas Sci. Eng.* **35** (SI part B) 1480 (2016)
94. Yu F Makogon *Gazovye Gidraty, Preduprezhdenie ikh Obrazovaniya i Ispol'zovanie* (Gas Hydrates, Prevention of Their Formation and Use) (Moscow: Nedra, 1985)
95. E M Freer, M S Selim, E D Sloan *Fluid Phase Equilib.* **185** 65 (2001)
96. M Sugaya, Y H Mori *Chem. Eng. Sci.* **51** 3505 (1996)

97. R Ohmura, S Kashiwazaki, Y H Mori *J. Cryst. Growth* **218** 372 (2000)
98. S Hirai, Y Tabe, K Kuwano, K Ogawa, K Okazaki, in *Gas Hudrates: Challenges for the Future (Ser. Annals of the New York Academy of Sciences* (New York: New York Acad. Sci., 2000) Vol. 9 (2), p. 246
99. R Ohmura, T Shigetomi, Y H Mori *J. Cryst. Growth* **196** 164 (1999)
100. B Z Peng, A Dandekar, C Y Sun, H Luo, Q L Ma, W X Pang, G J Chen *J. Phys. Chem. B* **111** 12485 (2007)
101. M Kitamura, Y H Mori *Cryst. Res. Technol.* **48** 511 (2013)
102. K Imasato, H Tokutomi, R Ohmura *Cryst. Growth. Des.* **15** 428 (2015)
103. C-Y Sun, G-J Chen, C-F Ma, Q Huang, H Luo, Q-P Li *J. Cryst. Growth* **306** 491 (2007)
104. Y H Mori *J. Cryst. Growth* **223** 206 (2001)
105. R Tanaka, R Sakemoto, R Ohmura *Cryst. Growth Des.* **9** 2529 (2009)
106. P Englezos, N Kalogerakis, P Dholabhai, P R Bishnoi *Chem. Eng. Sci.* **42** 2647 (1987)
107. M A Clarke, P R Bishnoi *Chem. Eng. Sci.* **60** 695 (2005)
108. F Al-Otaibi, M Clarke, B Maini, P R Bishnoi *Energy Fuels* **24** 5012 (2010)
109. F Al-Otaibi, M Clarke, B Maini, P R Bishnoi *Chem. Eng. Sci.* **66** 2468 (2011)
110. C Giraldo, B Maini, R Bishnoi, M Clarke *Energy Fuels* **27** 1204 (2013)
111. S Hashemi, A Macchi, P Servio *Ind. Eng. Chem. Res.* **46** 5907 (2007)
112. S Bergeron, P Servio *Fluid Phase Equilib.* **265** 30 (2008)
113. S Bergeron, P Servio *AIChE J.* **54** 2964 (2008)
114. S Bergeron, P Servio *Fluid Phase Equilib.* **276** 150 (2009)
115. S Bergeron, J G Beltran, P Servio *Fuel* **89** 294 (2010)
116. J Verrett, P Servio *Can. J. Chem. Eng.* **94** 2138 (2016)
117. P Skovborg, P Rasmussen *Chem. Eng. Sci.* **49** 1131 (1994)
118. J M Herri, J S Pic, F Gruy, M Cournil *AIChE J.* **45** 590 (1999)
119. R E T Meindinyo, T M Svartaas, T N Nordbu, R Bue *Energy Fuels* **29** 587 (2015)
120. N Gnanendran, R Amin *Chem. Eng. Sci.* **59** 3849 (2004)
121. M R Talaghat, F Esmaeilzadeh, J Fathikaljahi *Fluid Phase Equilib.* **279** 28 (2009)
122. A A Kendoush, K A Joudi, N A Jassim *Exp. Therm. Fluid Sci.* **30** 643 (2006)
123. Y-T Luo, J-H Zhu, S-S Fan, G-J Chen *Chem. Eng. Sci.* **62** 1000 (2007)
124. S Hashemi, A Macchi, P Servio *Chem. Eng. Sci.* **64** 3709 (2009)
125. S Matsuda, H Tsuda, Y H Mori *AIChE J.* **52** 2978 (2006)
126. D Yang, L A Le, R J Martinez, R P Currier, D F Spencer, G Deppe *Energy Fuels* **22** 2649 (2008)
127. L Cai, B A Pethica, P G Debenedetti, S Sundaresan *Chem. Eng. Sci.* **119** 147 (2014)
128. R E T Meindinyo, T M Svartaas *Energies* **9** 1201 (2016)
129. H K Abay, T M Svartaas, W Ke *Energy Fuels* **25** 1335 (2011)
130. J D Lee, R Susilo, P Englezos *Energy Fuels* **19** 1008 (2005)
131. P Linga, M A Clarke *Energy Fuels* **31** 1 (2017)
132. M Clarke, P R Bishnoi *Chem. Eng. Sci.* **55** 4869 (2000)
133. M Clarke, P R Bishnoi *Chem. Eng. Sci.* **56** 4715 (2001)
134. M Clarke, P R Bishnoi *Chem. Eng. Sci.* **59** 2983 (2004)
135. M Clarke, P R Bishnoi *Can. J. Chem. Eng.* **79** 143 (2001)
136. G C Nihous, K Kuroda, J R Lobos-Gonzalez, R J Kurasaki, S M Masutani *Chem. Eng. Sci.* **65** 1748 (2010)
137. T Kawamura, Y Sakamoto, M Ohtake, Y Yamamoto, T Komai, H Haneda *Ind. Eng. Chem. Res.* **45** 360 (2006)
138. M Liang, G Chen, C Sun, L Yan, J Liu, Q Ma *J. Phys. Chem. B* **109** 19034 (2005)
139. C Windmeier, L R Oellrich *J. Phys. Chem. A* **117** 12184 (2013)
140. C Windmeier, L R Oellrich *J. Phys. Chem. A* **117** 10151 (2013)
141. A V Egorov, G G Tsypkin *Fluid Dynam.* **34** 144 (1999)
142. A V Egorov, K Crane, P R Vogt, A N Rozhkov, P P Shirshov *Geo-Marine Lett.* **19** 68 (1999)
143. G Rehder, S H Kirby, W B Durham, L A Stern, E T Peltzer, J Pinkston, P G Brewer *Geochim. Cosmochim. Acta* **68** 285 (2004)
144. K C Hester, E T Peltzer, P M Walz, R M Dunk, E D Sloan, P G Brewer *Geochim. Cosmochim. Acta* **73** 6747 (2009)
145. G C Nihous, S A Masutani *Chem. Eng. Sci.* **61** 7827 (2006)
146. N K Bigalke, G Rehder, G Gust *Marine Chem.* **115** 226 (2009)
147. H J Hong, C H Ko, M H Song, S Lee, K Seong *J. Ind. Eng. Chem.* **41** 183 (2016)
148. Z Yin, Z R Chong, H K Tan, P Ling *J. Nat. Gas Sci. Eng.* **35** (SI part B) 1362 (2016)
149. T Jakobsen, J Sjoblom, P Ruoff *Colloids Surf., A* **112** 73 (1996)
150. L Mu, S Li, Q-L Ma, K Zhang, C-Y Sun, G-J Chen, B Liu, L-Y Yang *Fluid Phase Equilib.* **362** 28 (2014)
151. X Li, C Chen, Y Chen, Y Li, H Li *Energy Fuels* **29** 2277 (2015)
152. O B Kutergin, V P Mel'nikov, A N Nesterov *Dokl. Akad. Nauk* **323** 549 (1992)
153. P Gayet, C Dicharry, G Marion, A,Graciaa, J Lachaise, A Nesterov *Chem. Eng. Sci.* **60** 5751 (2005)
154. J D Botimer, D Dunn-Rankin, P Taborek *Chem. Eng. Sci.* **142** 89 (2016)
155. K Okutani, Y Kuwabara, Y H Mori *Chem. Eng. Sci.* **63** 183 (2008)
156. S Lee, J S Zhang, R Mehta, T K Woo, J W Lee *J. Phys. Chem. C* **111** 4734 (2007)
157. A Mandal, S Laik *Energy Fuels* **22** 2527 (2008)
158. J S Zhang, C Lo, P Somasundaran, S Lu, A Couzis, J W Lee *J. Phys. Chem. C* **112** 12381 (2008)
159. U Karaaslan, M Parlaktuna *Energy Fuels* **14** 1103 (2000)
160. F Long, S S Fan, Y H Wang, X M Lang *J. Nat. Gas Chem.* **19** 251 (2010)
161. T Daimaru, A Yamasaki, Y Yanagisawa *J. Petrol. Sci. Eng.* **56** 89 (2007)
162. U Karaaslan, E Uluneye, M Parlaktuna *J. Petrol. Sci. Eng.* **35** (1 – 2) 49 (2002)
163. N Ando, Y Kuwabara, Y H Mori *Chem. Eng. Sci.* **73** 79 (2012)
164. D Daniel-David, F Guerton, C Dicharry, J-P Torrè, D Broseta *Chem. Eng. Sci.* **132** 118 (2015)
165. A Kumar, G Bhattacharjee, B D Kulkarni, R Kumar *Ind. Eng. Chem. Res.* **54** 12217 (2015)
166. N N Nguyen, A V Nguyen *Fuel* **156** 87 (2015)
167. F Farhang, A V Nguyen, M A Hampton *Energy Fuels* **28** 1220 (2014)
168. G Bhattacharjee, N Choudhary, A Kumar, S Chakrabarty, R Kumar *J. Nat. Gas Sci. Eng.* **35** (SI part B) 1453 (2016)
169. H P Veluswamy, A Kumar, R Kumar, P Linga *Appl. Energy* **188** 190 (2017)
170. J Amtawong, J Guo, J S Hale, S Sengupta, E B Fleischer, R W Martin, K C Janda *J. Phys. Chem. Lett.* **7** 2346 (2016)
171. M A Kelland *Energy Fuels* **20** 825 (2006)
172. A Perrin, O M Musa, J W Steed *Chem. Soc. Rev.* **42** 1996 (2013)
173. E Abrahamsen, M Kelland *Energy Fuels* **30** 8134 (2016)
174. M A Kelland, W Ke *Energy Fuels* **30** 10015 (2016)
175. L Del Villano, R Kommedal, M A Kelland *Energy Fuels* **22** 3143 (2008)
176. H Bruusgaard, L D Lessard, P Servio *Cryst. Growth Des.* **9** 3014 (2009)
177. R Kumar, J D Lee, M Song, P Englezos *J. Cryst. Growth* **310** 1154 (2008)

178. J S Zhang, C Lo, A Couzis, P Somasundaran, J Wu, J W Lee *J. Phys. Chem. C* **113** 17418 (2009)
179. H Zeng, H L Lu, E Huva, V K Walker, J A Ripmeester *Chem. Eng. Sci.* **63** 4026 (2008)
180. R Gordienko, H Ohno, V K Singh, Z C Jia, J A Ripmeester, V K Walker *PLoS ONE* **5** e8953 (2010)
181. H Zeng, V K Walker, J A Ripmeester *Angew. Chem., Int. Ed.* **46** 5402 (2007)
182. H Zeng, I L Moudrakovski, J A Ripmeester, V K Walker *AIChE J.* **52** 3304 (2006)
183. J D Lee, H J Wu, P Englezos *Chem. Eng. Sci.* **62** 6548 (2007)
184. N Daraboina, P Linga, J Ripmeester, W K Walker, P Englezos *Energy Fuels* **25** 4384 (2011)
185. L Jensen, H Ramlov, K Thomsen, N von Solms *Ind. Eng. Chem. Res.* **49** 1486 (2010)
186. N Daraboina, I L Moudrakovski, J Ripmeester, W K Walker, P Englezos *Fuel* **105** 630 (2013).
187. D Posteraro, J Verrett, M Maric, P Servio *Chem. Eng. Sci.* **126** 99 (2015)
188. D Posteraro, J Ivall, M Maric, P Servio *Chem. Eng. Sci.* **126** 91 (2015)
189. N Daraboina, J Ripmeester, W K Walker, P Englezos *Energy Fuels* **25** 4392 (2011)
190. N Daraboina, J Ripmeester, W K Walker, P Englezos *Energy Fuels* **25** 4398 (2011)
191. X Wang, A J Schultz, Y Halpern *J. Phys. Chem. A* **106** 7304 (2002)
192. D S Staykova, W F Kuhs, A N Salamatin, T Hansen *J. Phys. Chem. B* **107** 10299 (2003)
193. W F Kuhs, D S Staykova, A N Salamatin *J. Phys. Chem. B* **110** 13283 (2006)
194. A Falenty, A N Salamatin, W F Kuhs *J. Phys. Chem. C* **117** 8443 (2013)
195. R M Barrer, F R S Edge, A V J Edge *Proc. Roy. Soc. London, Ser. A* **300** 1 (1967)
196. B J Farabella, M Vanpee *Ind. Eng. Chem. Fund.* **13** 228 (1974)
197. I L Moudrakovski, A A Sanchez, C I Ratcliffe, J A Ripmeester *J. Phys. Chem. B* **105** 12338 (2001)
198. R A Kini, S F Dec, E D Sloan *J. Phys. Chem. A* **108** 9550 (2004)
199. V S Yakushev *Eksperimental'noe Izuchenie Kinetiki Dissotsiatsii Gidrata Metana pri Otritsatel'nykh Temperaturakh* (Experimental Study of the Dissociation Kinetics of Methane Hydrate at Negative Temperatures) *EI VNIIGazprom (Ser. Razrabotka i Ekspluatatsiya Gazovykh i Gazokondensatnykh Mestorozhdenii)* **4** 11 (1988)
200. E D Ershov, Yu P Lebedenko, E M Chuvilin, V A Istomin, V S Yakushev *Dokl. Akad. Nauk* **321** 788 (1991)
201. V A Istomin, V S Yakushev, N A Makhonina, V G Kvon, E M Chuvilin *Gazovaya Prom-st'. Spets. Vypusk 'Gazovye Gidraty'* 36 (2006)
202. L A Stern, S Circone, S H Kirby, W B Durham *J. Phys. Chem. B* **105** 1756 (2001)
203. S Takeya, T Uchida, J Nagao, R Ohmura, W Shimada, Y Kamata, T Ebinuma, H Narita *Chem. Eng. Sci.* **60** 1383 (2005)
204. S Takeya, W Shimada, Y Kamata, T Ebinuma, T Uchida, J Nagao, H Narita *J. Phys. Chem. A* **105** 9756 (2001)
205. W Shimada, S Takeya, Y Kamata, T Uchida, J Nagao, T Ebinuma, H Narita *J. Phys. Chem. B* **109** 5802 (2005)
206. S Takeya, T Ebinuma, T Uchida, J Nagao, H Narita *J. Cryst. Growth* **237** – **239** 379 (2002)
207. Y P Handa *J. Chem. Thermodyn.* **18** 891 (1986)
208. V S Yakushev, V A Istomin, in *Physics and Chemistry of Ice* (Sapporo: Hokkaido University Press, 1992) p. 136
209. A Falenty, W F Kuhs, M Glockzin, G Rehder *Energy Fuels* **28** 6275 (2014)
210. T Uchida, M Kida, J Nagao *ChemPhysChem* **12** 1652 (2011)
211. V P Mel'nikov, A N Nesterov, A M Reshetnikov *Dokl. Earth Sci. A* **389** 455 (2003)]
212. K Takeya, K Nango, T Sugahara, K Ohgaki, A Tani *J. Phys. Chem. B* **109** 21086 (2005)
213. H Ohno, H Narita, J Nagao *J. Phys. Chem. Lett.* **2** 201 (2011)
214. E A Smelik, H E King Jr *Am. Mineral.* **82** 88 (1997)
215. A S Stoporev, A Yu Manakov, L K Altunina, L A Strelets, V I Kosyakov *Can. J. Chem.* **93** 882 (2015)
216. G D Ginsburg, V A Solov'ev *Submarinnye Gazovye Gidraty* (Submarine Gas Hydrates) (Moscow: VNIIOkeangeologiya, 1994)
217. D Dalmazzone, H Hamed, C Dalmazzone *Chem. Eng. Sci.* **64** 2020 (2009)
218. D Dalmazzone, H Hamed, C Dalmazzone, L Rousseau *J. Therm. Anal. Calorim.* **85** 361 (2006)
219. M S Madygulov, A N Nesterov, A M Reshetnikov, V A Vlasov, A G Zavodovsky *Chem. Eng. Sci.* **137** 287 (2015)
220. A K Sum, R C Burruss, E D Sloan Jr *J. Phys. Chem. B* **101** 7371 (1997)
221. C A Tulk, J A Ripmeester, D D Klug, in *Gas Hydrates: Challenges for the Future (Ser. Annals of the New York Academy of Sciences)* (New York: New York Acad. Sci., 2000) Vol. 912, p. 859
222. P Servio, P Englezos, P R Bishnoi, in *Gas Hydrates: Challenges for the Future (Ser. Annals of the New York Academy of Sciences)* (New York: New York Acad. Sci., 2000) Vol. 912, p. 576
223. J S Parent, P R Bishnoi, in *Gas Hydrates: Challenges for the Future (Ser. Annals of the New York Academy of Sciences)* (New York: New York Acad. Sci., 1994) Vol. 715, p. 552
224. J P Monfort, A Nzihou *J. Cryst. Growth.* **128** 1182 (1993)
225. C Sun, G Chen, T Guo *Sci. China, Ser. B* **46** 488 (2003)
226. J M Herri, F Gruy *Mater. Chem. Phys.* **42** 51 (1995)
227. M Bylov, P Rasmussen *Chem. Eng. Sci.* **52** 3295 (1997)
228. V P Mel'nikov, A N Nesterov, V V Feklistov *Zh. Fiz. Khim.* **76** 1318 (2001)
229. M H Yousif, R B Dorshow, D B Young, in *Gas Hydrates: Challenges for the Future (Ser. Annals of the New York Academy of Sciences)* (New York: New York Acad. Sci., 1994) Vol. 715, p. 330
230. T Uchida, R Ohmura, J Nagao *J. Chem. Eng. Data.* **48** 1225 (2003)